Adaptive-depth randomized measurement for fermionic observables

Kaiming Bian[1, 2, 3] and Bujiao Wu[1, 2, 3, *]

[1] *Shenzhen Institute for Quantum Science and Engineering, Southern University of Science and Technology, Shenzhen 518055, China*
[2] *International Quantum Academy, Shenzhen 518048, China*
[3] *Guangdong Provincial Key Laboratory of Quantum Science and Engineering, Southern University of Science and Technology, Shenzhen, 518055, China*

...

I. INTRODUCTION

Simulation of strongly correlated fermionic systems is one of the most important applications of quantum computing [1, 2], highlighting the necessity for advanced measurement techniques in fermionic systems to capture the intricacies of electron correlations and dynamics. An important example of this is the k-reduced density matrix (k-RDM), which efficiently captures the essential features of many-body fermionic systems by focusing on a subset of particles and involves the calculation of various expectation values of fermionic observables. It demonstrates the importance of the efficient calculations of the expectation values in fermionic systems.

The classical shadow (CS) algorithm [3] was introduced to give a classical estimator for a quantum state ρ by employing a random Clifford circuit, measurement in the computational basis, and polynomial classical postprocessing. It is particularly suited for estimating linear properties of ρ, such as the expectation values $\{\mathrm{Tr}\left(\rho Q_i\right)\}_{i=1}^{m}$. The number of measurements required is $\mathcal{O}\left(\max_i \|Q_i\|_{\mathrm{shadow}}^2 \log m/\varepsilon^2\right)$, where ε is the desired estimation error and $\|\cdot\|_{\mathrm{shadow}}$ denotes the shadow norm, which depends on the choice of the unitary ensemble. When the unitary ensemble is the global Clifford group, the shadow norm simplifies to $\|Q\|_{\mathrm{shadow}} = \mathrm{Tr}\left(Q^2\right)$. Although it is efficient for k-local Pauli observables, it is not efficient for k-local fermionic observables, such as Majorana operators. To address this limitation, fermionic classical shadow (FCS) algorithms [4–6] were developed. These algorithms primarily differ from the CS algorithm by using a Gaussian unitary ensemble rather than the Clifford group for randomness. Both Gaussian unitary and Clifford elements require polynomial-size quantum circuits, which become challenging for near-term quantum devices due to issues like gate noise and limited coherence time [7–12]. In response to this, several approaches have been proposed to design shallow-depth CS protocols [13–15]. However, for FCS side, Zhao et al. [4] have proved that there does not exist subgroup $G \subset \mathrm{Cl}_n \cap \mathbb{M}_n$ which has a better fermionic shadow norm, where Cl_n is the n-qubit Clifford group and $\mathbb{M}_n$ is the matchgate group. An intriguing open question remains:

Is there a shallow-depth FCS algorithm that is efficient for some specific set of fermionic observables and maintains the same sample complexity as the original FCS algorithm?

In this study, we delve into the relationship between sample complexity and the depth utilized in constructing the random unitary ensemble. Our analysis focuses on the 1-RDM, leading to an expression that characterizes the connection between sample complexity and the number of layers. Then, we find the relationship for the k-RDM that aligns well with experimental observations. Based on the findings, we investigated the requisite depth of layers necessary to achieve the minimal sample number. Notably, the requisite depth is tight in order, indicating that attaining the same lower bound with fewer layers is impossible, thereby providing significant insight into optimizing the depth of random unitary ensembles for practical quantum computing applications.

II. PRELIMINARY

Notations. We utilize $\mathcal{H}$ to denote the quantum state Hilbert space, and $\mathcal{L}(\mathcal{H})$ to denote the linear operator space which operates on Hilbert space $\mathcal{H}$. Quantum channel $\Lambda \in \mathcal{L}(\mathcal{L}(\mathcal{H}))$ is a superoperator that maps a linear operator into another. For convenience, we introduce the Pauli-transfer matrix (PTM) representation, which expresses both superoperators and operators in terms of their action on the Pauli basis. A non-zero linear operator $|A\rangle\rangle$ can be

* wubj@sustech.edu.cn

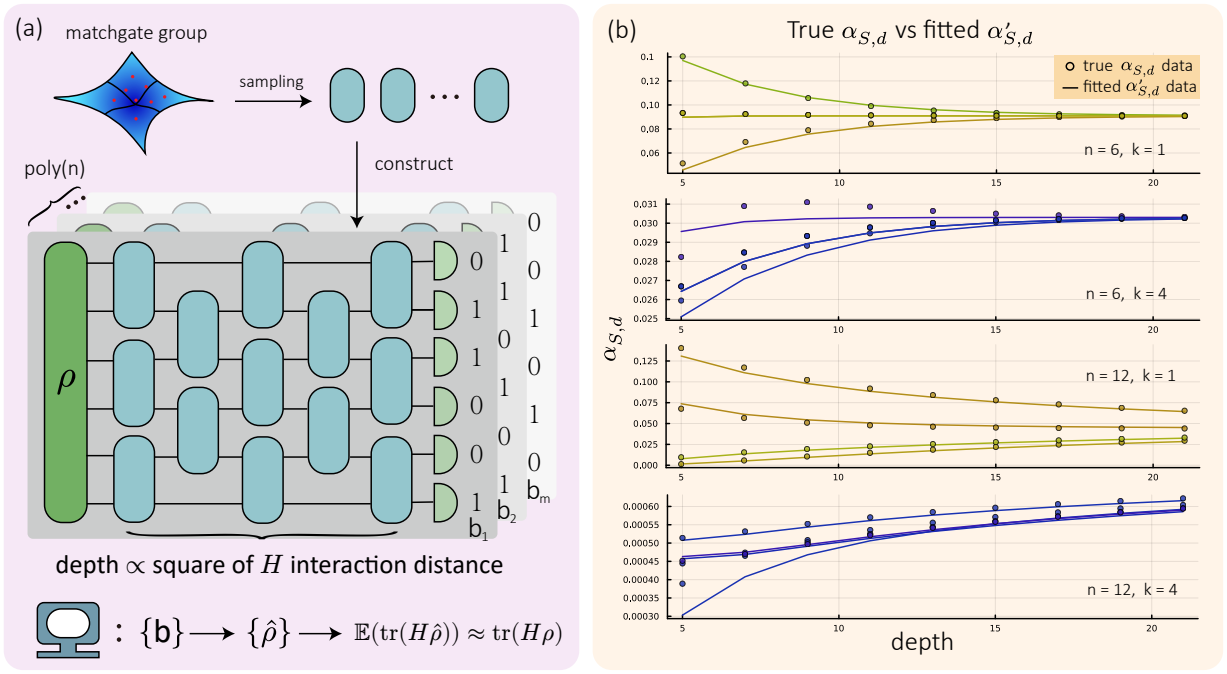

FIG. 1: Illustration of adaptive depth fermionic shallow shadows (ADFCS). (a) The sketch of ADFCS. Unitary gates are independently sampled from the group of two-qubit matchgates and subsequently assigned to each node within the brickwork architecture. Measuring the constructed random circuit multiple times yields a set of bit strings $\{b\}$, which can then be processed on a classical computer. This post-processing step estimates $\mathrm{tr}(H\rho)$ by averaging the expectation values of the classical shadows $\{\hat{\rho}\}$ derived from bit strings $\{b\}$. Depending on the fitting formula of $\alpha_{S,d}$ in Eq. (25), the sampling complexity remains efficient, ensuring the feasibility of the computational process when the depth of random measurement circuit scales proportionally to the square of the interaction distance of the fermionic Hamiltonian $H = \sum c_S \gamma_S$. (b) illustrates the accuracy of the fit $\alpha'_{S,d}$ in comparison to the true value $\alpha_{S,d}$. The results demonstrate that the fitting aligns closely with the true values, particularly when the circuit depth is sufficiently large.

vectorized as $|A\rangle\rangle := \frac{A}{\sqrt{\mathrm{Tr}(A^\dagger A)}}$ where the normalization ensures that it is properly scaled. The inner product between the vectorized formation of two operators $A, B \in \mathcal{L}(\mathcal{H})$ is defined as $\langle\langle A|B\rangle\rangle := \frac{\mathrm{Tr}(A^\dagger B)}{\sqrt{\mathrm{Tr}(A^\dagger A)\mathrm{Tr}(B^\dagger B)}}$. Specifically, for the Majorana observable γ_S, the vectorized form is $|\gamma_S\rangle\rangle = \frac{\gamma_S}{\sqrt{2^n}}$, where n is the number of qubits. The superoperator Λ can be represented as a matrix in Pauli basis. Its operating on a linear operator $A \in \mathcal{L}(\mathcal{H})$ can be denoted as $\Lambda|A\rangle\rangle := \frac{\Lambda(A)}{\sqrt{\mathrm{Tr}(A^\dagger A)}}$. Further details on the Pauli-transfer matrix representation can be found in Appendix A.

Majorana operators and matchgate circuits. Studying Majorana operators in fermionic systems is crucial as they underpin the behavior of these systems and have numerous applications, including calculating the expectation values of Majorana operators, such as the energy related to the fermionic Hamiltonian and all elements of k-RDM. The Majorana operators can be defined as

$$\gamma_{2j-1} := a_j + a_j^\dagger, \quad \gamma_{2j} := -\mathrm{i}\left(a_j - a_j^\dagger\right), \tag{1}$$

where $a_j, a_j^\dagger$ are the annihilation and creation operators for the j-th site respectively. Observables in fermionic systems can be expressed as the linear combination of the products of Majorana operators [16]

$$\gamma_S := \gamma_{i_1}\gamma_{i_2}\cdots\gamma_{i_{|S|}}, \tag{2}$$

where $i_1 < i_2 < \cdots < i_{|S|}$, and $S = \{i_1, i_2, \cdots, i_{|S|}\}$. Especially, we set $\gamma_\emptyset$ be the identity operator $\mathbb{1}$ when S is the empty set $\emptyset$. A Majorana operator can be represented in Pauli formation as $\gamma_{2j-1} = \left(\prod_{i=1}^{j-1} Z_i\right) X_j$, $\gamma_{2j} = \left(\prod_{i=1}^{j-1} Z_i\right) Y_j$, for any $j \in [2n]$.

Except for the standard Majorana operators in Eq. (1), there are different bases to express the fermionic Hamiltonian. Different bases could be obtained by the orthogonal transformation of the standard Majorana operators $\tilde{\gamma}_\mu = \sum_{\nu=1}^{2n} Q_{\mu\nu}\gamma_\nu$, where Q is a real orthogonal matrix, $Q \in O(2n)$. The different sets of bases $\{\tilde{\gamma}_\mu\}$ are also called the Majorana operators because they satisfy the same anti-commutation relation $\{\gamma_\nu, \gamma_\mu\} = 2\delta_{\mu\nu}$. The orthogonal linear combinations of Majorana operators can be represented as unitary

$$U_Q^\dagger \gamma_\mu U_Q = \sum_{\nu=1}^{2n} Q_{\mu\nu}\gamma_\nu = \tilde{\gamma}_\mu, \tag{3}$$

where the unitaries U_Q are called fermionic Gaussian unitaries. Followed by Eq. (3), the fermionic Gaussian unitary preserves the cardinality $|S| = \#\{i \mid i \in S\}$ of γ_S, which can be expressed as $U_Q^\dagger \gamma_S U_Q = \sum_{|S'|\in\binom{[2n]}{|S|}} \det\left(Q|_{S,S'}\right)\gamma_{S'}$. The set $\binom{[2n]}{|S|}$ represents the collection of all subsets of $\{1, 2, \ldots, 2n\}$ that contain exactly $|S|$ elements, and the matrix $A|_{S,S'}$ is obtained from the matrix A by selecting the rows indexed by the set S and the columns indexed by the set S'.

Matchgate circuits are the quantum circuit representation of fermionic Gaussian unitaries [6]. The collection of all n-qubit matchgate circuits constitutes the matchgate group $\mathbb{M}_n$. This group is generated by rotations of the form $\exp\left(\mathrm{i}\theta X_\mu X_\nu\right), \exp\left(\mathrm{i}\theta Z_\mu\right)$ and X_n, where θ is a real parameter, and μ, ν are indices corresponding to nearest-neighbor qubits in a linear arrangement. Notably, operations within the matchgate group can be efficiently simulated on a classical computer. This efficiency arises because the action of a matchgate circuit U_Q corresponds to Givens rotations associated with an orthogonal matrix Q, facilitating polynomial-time classical simulation [9, 17].

We present the twirling of the matchgate group in the following lemma, as it is utilized in the proof of our main results.

Lemma 1 (The three moments of uniform distribution in $\mathbb{M}_n$, Ref. [6])**.** *The k-moment twirling $\mathcal{E}^{(j)}$ is defined by*

$$\mathcal{E}^{(j)}(\cdot) := \int_{U_Q\in\mathbb{M}_n} \mathrm{d}Q\; U_Q^{\otimes j}(\cdot)U_Q^{\dagger\otimes j}. \tag{4}$$

The first three moments are

$$\begin{aligned}
\mathcal{E}^{(1)} &= |\mathbb{1}\rangle\rangle\langle\langle\mathbb{1}| \\
\mathcal{E}^{(2)} &= \sum_{k=0}^{2n}\binom{2n}{k}^{-1} \sum_{S,S'\subseteq[2n]} |\gamma_S\rangle\rangle|\gamma_S\rangle\rangle\langle\langle\gamma_{S'}|\langle\langle\gamma_{S'}| \\
\mathcal{E}^{(3)} &= \sum_{\substack{k_1,k_2,k_3\in[2n]\\ k_1+k_2+k_3\le 2n}} |\mathcal{R}\rangle\rangle\langle\langle\mathcal{R}|,
\end{aligned} \tag{5}$$

where

$$|\mathcal{R}\rangle\rangle = \binom{2n}{k_1,k_2,k_3,2n-k_1-k_2-k_3}^{-1/2} \sum_{\substack{A,B,C\,disjoint\\ |A|=k_1,|B|=k_2,|C|=k_3}} |\gamma_A\gamma_B\rangle\rangle|\gamma_B\gamma_C\rangle\rangle|\gamma_C\gamma_A\rangle\rangle. \tag{6}$$

(Fermionic) classical shadow protocol. The classical shadow (CS) process involves randomly applying a unitary $\mathcal{U}$ from some unitary ensemble $\mathbb{U}$ (such as the Clifford group) on a quantum state ρ, followed by measurement in computational bases, yielding outcomes $|b\rangle\rangle$ that form a classical description of ρ, known as "*classical shadow*", denoted as $\hat{\rho} = \mathcal{M}_{\mathrm{CS}}^{-1}\mathcal{U}^{-1}|b\rangle\rangle$, where $\mathcal{M}_{\mathrm{CS}} := \mathbb{E}_{\mathcal{U}\in\mathbb{U}}\left[\mathcal{U}^\dagger \sum_b |b\rangle\rangle\langle\langle b|\mathcal{U}\right]$. By choosing $\mathbb{U}$ as Clifford group Cl_n, the classical shadow channel can be simplified to $\mathcal{M}_{\mathrm{CS}} = \Pi_0 + \frac{1}{2^n+1}\Pi_1$, where Π_0 is the projector onto the identity subspace and Π_1 is the projector onto the subspace spanned by all Pauli bases except identity [3, 18]. This simple representation allows efficient construction of the classical shadow $\hat{\rho}$.

In the framework of FCS, the shadow channel $\mathcal{M}_{\mathrm{FCS}} := \int_{Q\in O(2n)} \mathrm{d}Q\mathcal{U}_Q^\dagger \sum_b |b\rangle\rangle\langle\langle b|\mathcal{U}_Q$ is not invertible across the entire Hilbert space. Its invertibility is constrained to a subspace spanned by even operators, denoted as $\Gamma_{\mathrm{even}} := \mathrm{span}\{\gamma_S \mid |S| = 2j, j = 0, 1, 2, \cdots, n\}$. For set S with odd cardinality, the channel $\mathcal{M}_{\mathrm{FCS}}(\gamma_S) = 0$, rendering these components inaccessible.

As a result, FCS is limited to recovering expectation values of observables that reside within the Γ_{even} subspace. However, this restriction is sufficient for capturing physical observables, as they are typically even operators due to the conservation of fermionic parity [19]. Unless otherwise specified, all discussions and calculations are assumed to take place within the Γ_{even}.

III. ADAPTIVE-DEPTH FERMIONIC CLASSICAL SHADOWS

Here we consider the adaptive-depth fermionic classical shadow (ADFCS) by selecting the unitary ensemble as d-depth local matchgates with brickwork architecture, as shown in Fig. 1(a), which is widely applied in superconducting quantum devices [10]. It has been shown that certain observables cannot be addressed by replacing the global $\mathrm{Cl}_n \cap \mathbb{M}_n$ group with shallow-depth local matchgate circuits [4]. However, it remains open when global elements are necessary and how to efficiently generate the expectation values of a given set of fermionic observables using the shallowest depth matchgate circuits while minimizing the number of samplings. Here, we address this question by exploring the relationship between the number of required measurements and the depth of the matchgate circuit for some specific set of fermionic observables using the brickwork architecture. Our approach introduces a d-depth ADFCS channel to estimate $\mathrm{Tr}(\rho\gamma_S)$ for any quantum state ρ. We then determine the optimized depth order for the expectation values of the specific fermionic observables $\mathrm{Tr}(\rho\gamma_S)$ with respect to an unknown quantum state ρ prepared by a quantum device.

A. Shadow channel in ADFCS

For simplicity, we utilize U_{Q_d} to denote a d-depth matchgate circuit with brickwork structure, and $\mathbb{U}_{Q_d}$ to denote the set of all d-depth matchgate circuit throughout this manuscript. We denote $\mathcal{M}_d$ as the d-depth ADFCS shadow channel, which maps a quantum state ρ to

$$\mathcal{M}_d(\rho) := \mathop{\mathbb{E}}_{U\in\mathbb{U}_{Q_d}, b\in\{0,1\}^n} \left[\langle b| U_{Q_d}\rho U_{Q_d}^\dagger |b\rangle U_{Q_d}^\dagger |b\rangle \langle b| U_{Q_d} \right]. \tag{7}$$

By the property of the average of $\mathbb{U}_{Q_d}$, we see that the Majorana operator is invariant under the operation of $\mathcal{M}_d$ up to a coefficient $\alpha_{S,d}$

$$\mathcal{M}_d(\gamma_S) = \alpha_{S,d}\gamma_S, \tag{8}$$

where $\alpha_{S,d} := \int \mathrm{d}U_{Q_d} \left| \langle 0| U_{Q_d}\gamma_S U_{Q_d}^\dagger |0\rangle \right|^2$. The proof is shown in the Appendix. B.

Eq. (8) gives the shadow channel's concrete expression, enabling us to analyze various statistical properties of ADFCS. The ADFCS with d-layer shadow channel $\mathcal{M}_d$ is an unbiased estimator like FCS. The ADFCS estimator is unbiased because of the linearity of channel $\mathcal{M}_d$

$$\mathop{\mathbb{E}}_{U_{Q_d},b} (\mathcal{M}_d^{-1}(U_{Q_d}^\dagger |b\rangle \langle b| U_{Q_d})) = \mathcal{M}_d^{-1}(\mathbb{E}(U_{Q_d}^\dagger |b\rangle \langle b| U_{Q_d})) = \rho. \tag{9}$$

Eq. (9) shows the average of classical shadows $\hat{\rho}$ equal to the origin state ρ, thereby using the ADFCS to estimate the expectation value of any observable in Γ_{even} is unbiased.

Due to the sampling distribution and Chebyshev inequality, the sample complexity is determined by the variance. The larger the variance, the more dispersed the data and, consequently, the larger the required sample size. Given any observable γ_S and an unknown quantum state ρ, the variance of ADFCS estimator is bounded by $1/\alpha_{S,d}$,

$$\mathrm{Var}[v] \le \frac{1}{\alpha_{S,d}}, \tag{10}$$

where the estimator v is the random variable $\mathrm{Tr}(\hat{\rho}\gamma_S)$. We show the calculation of Eq. (10) in Appendix C. Notice that the bond is tight because there always exists state ρ such that the variance $\mathrm{Var}[v]$ equals $\frac{1}{\alpha_{S,d}}$. In this case, the $\alpha_{S,d}$ order will directly determine the variance order. Hence, the order of $\alpha_{S,d}$ determines the sample complexity.

B. Represent $\alpha_{S,d}$ in tensor network

We will begin with the definition of $\alpha_{S,d}$ and proceed to estimate its order. To simplify the representation of the unitary transformation, we represent the unitary transformation of Majorana operators as the action of superoperators on supervectors

$$\left(U_{Q_d}\gamma_S U_{Q_d}^\dagger\right) \otimes \left(U_{Q_d}\gamma_S U_{Q_d}^\dagger\right) \to \mathcal{U}_{Q_d}|\gamma_S,\gamma_S\rangle\rangle. \tag{11}$$

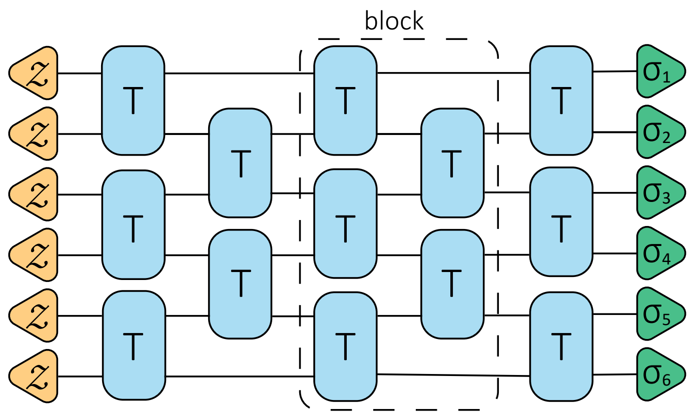

FIG. 2: Tensor network representation of $\alpha_{S,d}$. Each blue square represents tensor T, which is shown in Eq. 13. The green triangles compose the Pauli operator $\sigma_1 \otimes \cdots \otimes \sigma_n$ corresponding to the Majorana operator γ_S. The yellow triangles represent the supervector $|\mathcal{Z}\rangle\rangle = \frac{1}{2}(|I,I\rangle\rangle + |Z,Z\rangle\rangle)$.

After reformulation, alpha takes the form of a superoperator's expectation value

$$\alpha_{S,d} = \langle\langle 0,0| \int \mathrm{d}U_{Q_d} \mathcal{U}_{Q_d} |\gamma_S, \gamma_S\rangle\rangle. \tag{12}$$

Notice that the unitary $\mathcal{U}_{Q_d}$ is composed of the multiplication of independent 2-qubit matchgates $\mathcal{U}_{Q_2}$. Consequently, the integration over U can be broken down into a product of a series of integrations over these independent 2-qubit matchgates. Ref. [6] gives the close form of the integration over 2-qubit matchgates, which can be expressed as a 4-order tensor T

$$T^{\sigma_1,\sigma_2}_{\sigma_3,\sigma_4} := \langle\langle \sigma_1, \sigma_2 | \langle\langle \sigma_1, \sigma_2 | \int \mathrm{d}U_{Q_2} \mathcal{U}_{Q_2} |\sigma_3, \sigma_4\rangle\rangle |\sigma_3, \sigma_4\rangle\rangle, \tag{13}$$

where $\sigma_1, \sigma_2, \sigma_3, \sigma_4$ are Pauli operators. By connecting these tensors T in the same architecture as U_{Q_d}, as shown in Fig. **??**, the integration over the superoperator can be transformed into a tensor network. And the details of the transformation are shown in Appendix D.

The tensor network representation of $\alpha_{S,d}$ is depicted in Fig. 2. Notably, the basis of tensor T consists of Pauli operators. Therefore, to compute $\alpha_{S,d}$, the supervectors $|\gamma_S, \gamma_S\rangle\rangle$ and $\langle\langle 0,0|$ need to be expressed in the Pauli basis. Specifically, the supervectors $|\gamma_S, \gamma_S\rangle\rangle$ can be represented in the Pauli basis using the Jordan-Wigner transformation, while $\langle\langle 0,0|$ corresponds to $(|Z,Z\rangle\rangle + |I,I\rangle\rangle)^{\otimes n}$. This approach reformulates $\alpha_{S,d}$ as the contraction of a tensor network

$$\alpha_{S,d} = \langle\langle 0,0| T_{\text{whole}} |\gamma_S, \gamma_S\rangle\rangle, \tag{14}$$

where T_{whole} is the whole T tensor network (the whole blue part in Fig. 2).

C. The order of $\alpha_{S,d}$ for 1-RDM

In extreme cases, the scaling behavior of $\alpha_{S,d}$ can be determined. The variable $\alpha_{S,0}$ is zero for most observables when the circuit depth is 0; and when the depth goes to infinity, the ADFCS devolves to FCS and the $\alpha_{S,\infty}$ is in the order of $\frac{1}{\mathrm{poly}(n)}$. As the number of layers increases, $\alpha_{S,d}$ grows from 0 to $\frac{1}{\mathrm{poly}(n)}$. Since the sampling complexity is inversely proportional to $\alpha_{S,d}$, it decreases to a polynomial scale as the layer count increases.

Our goal is to investigate the scale of layer depth at which the sampling complexity transitions from an exponential scale to a polynomial scale. To identify the layer order for efficient measurement, we derive an expression of $\alpha_{S,d}$ and determine the depth d^* such that $\alpha_{S,d^*} = \frac{1}{\mathrm{poly}(n)}$.

Estimating this order using tensor network contraction in mesoscopic depth is challenging. However, we could simplify the calculation by restricting the action of the tensor within the subspace spanned by 1-RDM

$$\Gamma_1 := \mathrm{span}\{\gamma_S \mid |S| = 2\}. \tag{15}$$

By restricting the action of tensor T to the subspace Γ_1, we can introduce more refined structures by mapping this subspace to a polynomial space. This isomorphism allows us to analyze the system more effectively. In this context, the tensor network contraction of $\alpha_{S,d}$ is equivalent to a random walk in the polynomial space.

The effective subspace can be further simplified by expressing the circuits in a standard form. Assume the qubit count n is even, and the circuit depth d is odd. Under these conditions, the action of tensor T on the circuit can be represented within the space of quadratic polynomials with $\frac{n}{2}$ variables. In this quadratic polynomial space $\mathcal{P}_{\frac{n}{2}}$, the action of T becomes sufficiently simple to uncover hidden phenomena.

The action of T in Γ_1 is equivalent to a random walk. Intuitively, the action of a block in Fig. 2 is a transition process

$$T_{\text{block}}|\gamma_S,\gamma_S\rangle\rangle = \sum_{|S'|=|S|} \text{Prob}(\gamma_{S'}|\gamma_S)|\gamma_S,\gamma_S\rangle\rangle, \tag{16}$$

where $\text{Prob}(\gamma_{S'}|\gamma_S)$ satisfies the normalization condition $\sum \text{Prob}(\gamma_{S'}|\gamma_S) = 1$. The operation of the overall T tensor can be understood as the repeated application of T_{block} to γ_S

$$T_{\text{whole}} = T_{\text{block}}^{\lfloor \frac{d}{2} \rfloor} T_{\text{init}}, \tag{17}$$

where the T_{init} is the initiate layer of tensor T, $T_{\text{init}} := T^{\otimes \frac{n}{2}}$. Each T-block corresponds to a single step in a random walk. Therefore, the entire T tensor operation represents a random walk starting from γ_S and taking $\lfloor \frac{d}{2} \rfloor$ steps. The details of mapping the tensor contraction of $\alpha_{S,d}$ to the random walk in $\mathcal{P}_{\frac{n}{2}}$ is shown in Appendix E.

We observe that the random walk follows the pattern of a symmetry lazy random walk (SLRW) [20, 21] almost everywhere within the Γ_1 space. Firstly, we consider the SLRW across the subspace Γ_1 adheres to the SLRW

$$L_{\text{T}}|\gamma_S,\gamma_S\rangle\rangle = \sum_{|S'|=|S|} \text{Prob}_L(\gamma_{S'}|\gamma_S)|\gamma_S,\gamma_S\rangle\rangle. \tag{18}$$

And we calculate an $\alpha_{S,d}^L$ corresponding to SLRW pattern

$$\alpha_{S,d}^L = \langle\langle 0,0|L_{\text{T}}^{\lfloor \frac{d}{2} \rfloor} T_{\text{init}}|\gamma_S,\gamma_S\rangle\rangle. \tag{19}$$

Notice that in most places of subspace Γ_1, $L_{\text{T}} = T_{\text{block}}$. Compare with Eq. (19), it suggests that the variable $\alpha_{S,d}^L$ should be the dominant part of $\alpha_{S,d}$. Secondly, We show that this intuition is correct. The order of $\alpha_{S,d}$ and the trend of $\alpha_{S,d}$ are decided by $\alpha_{S,d}^L$.

There is a known analytical propagation equation for the SLRW [20]. By applying this propagation equation and making certain approximations, the α-value can ultimately be expressed as a Poisson summation

$$\alpha_{S,d}^L = \frac{1}{\sqrt{4\pi(d-1)}} \sum_{k=-\infty}^{\infty} \left(e^{-\frac{(kn+a)^2}{d-1}} + e^{-\frac{(kn+b)^2}{d-1}} \right) + \mathcal{O}(e^{-\frac{\pi^2 d}{2}}). \tag{20}$$

In Eq. (20), we denote the 1-RDM observable γ_S as $\gamma_i\gamma_j$, the variable a, b are defined by $a := |\lfloor \frac{i-1}{4} \rfloor - \lfloor \frac{j-1}{4} \rfloor|$, and $b := \lfloor \frac{i-1}{4} \rfloor + \lfloor \frac{j-1}{4} \rfloor + 1$. We leave the concrete detection of Eq. (20) to Appendix F.

Here, we move to the relationship between $\alpha_{S,d}^L$ and $\alpha_{S,d}$. Denote the difference between the true random walk and the SLRW as

$$\Delta(S,S',d) = \langle\langle \gamma_{S'},\gamma_{S'}|L_{\text{T}}^{\lfloor \frac{d}{2} \rfloor} T_{\text{init}}|\gamma_S,\gamma_S\rangle\rangle. \tag{21}$$

Recall that the operator $\gamma_{S'} = \gamma_{i_{S'}}\gamma_{j_{S'}}$ for 1-RDM. In numerical experiments, we find that the difference $\Delta(S,S',d)$ is positive if and only if the $i_{S'}$ is near the $j_{S'}$. Under this assumption, we prove that

$$\alpha_{S,d} \geq c\alpha_{S,d}^L \tag{22}$$

for a constant c. We show the experiment evidence and the proof in Appendix G.

As observed in Eq. (20), a measurement depth d can yield a sufficiently large $\alpha_{S,d}$ when a approaches 0. Conversely, if a is not close to 0, achieving a polynomially small $\alpha_{S,d}$ (rather than an exponentially small one) requires a depth of $d = \Omega\left(\frac{(i-j)^2}{\log(n)}\right)$. Thus, we could adaptively select the depth d based on the distance $|i-j|$,

$$d^* = \frac{(i-j)^2}{\log(n)}. \tag{23}$$

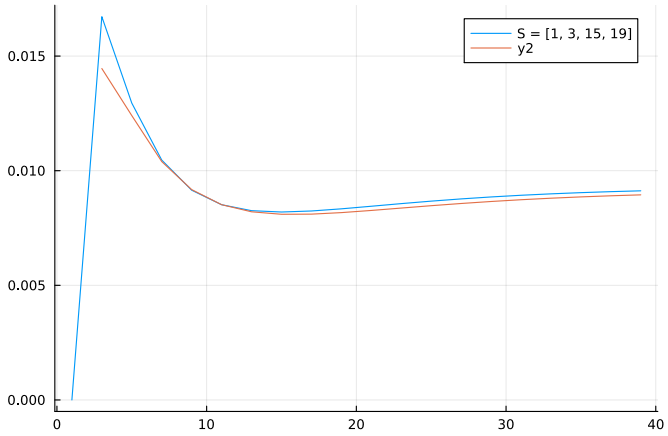

FIG. 3: Caption

Eq. (20) ensures that when we select depth d with lower orders, the value of $\alpha^L_{S,d}$ becomes exponentially small. It indicates that we need exponential samples to obtain the expectation value.

From numerical experiments, we observe that $c\alpha^L_{S,d}$ not only serves as a lower bound for $\alpha_{S,d}$ but also provides a close approximation to $\alpha_{S,d}$. We choose the coefficient c as

$$c = \lim_{d\to\infty} \frac{\alpha_{S,d}}{\alpha^L_{S,d}} = \frac{n}{2n-1}, \tag{24}$$

where the limitation of $\alpha_{S,d}$ is calculated by the closed expression of shadow channel in Ref. [6]. This coefficient ensures that $c\alpha^L_{S,d}$ will converge to $c\alpha^L_{S,d}$ when the depth goes to infinity. As shown in Fig. **??**, the curve of $c\alpha^L_{S,d}$ fits the points of $\alpha_{S,d}$.As shown in Fig. **??**, the curve of $c\alpha^L_{S,d}$ fits the $\alpha_{S,d}$ for shallow depth. Thus, we conclude that the $c\alpha^L_{S,d}$ is a good approximation of $\alpha_{S,d}$.

D. Fitting $\alpha_{S,d}$ for k-RDM

In this section, we address the extension of the results for 1-RDM to k-RDM. The situation for k-RDM differs significantly, as FCS becomes inefficient when k is large. Specifically, for $k = \mathcal{O}(n)$, $\alpha_{S,\infty}$ decreases exponentially, as noted in [4]. Thus, we focus on the case of constant k, as the sample complexity remains polynomial in this regime. Moreover, constant k is sufficient to capture many practical observables in quantum systems. This focus enables a balance between computational feasibility and practical applicability.

If the distance of any near neighborhood in S is small, we prove that a shallow measurement circuit is sufficient to make $\alpha_{S,d}$ as large as $\mathcal{O}(1/\text{poly}(n))$ for constant k. From Eq. (19) and Eq. (16), we conclude that the value of $\alpha_{S,d}$ is the sum of probabilities associated with specific sites after the random walk. When the distance of the near neighborhood $i_k, i_{k+1} \in S$ logarithmically small $|i_k - i_{k+1}| = \mathcal{O}(\log(n))$, a logarithmically transition steps can traverse from $|\gamma_S, \gamma_S\rangle\rangle$ to specific sites. Due to Eq. (16), each step introduces a constant probability factor. Thus, the probability of reaching specific sites is $\mathcal{O}(1/\text{poly}(n))$ after logarithmic steps random walk. We put the details of the proof in Appendix H.

However, the theoretical analysis of $\alpha_{S,d}$ becomes significantly more challenging if S lacks structures. We propose a general form for $\alpha_{S,d}$ based on the expression for the 1-RDM. Numerical experiments show that the proposed expression $\alpha'_{S,d}$ fits the true $\alpha_{S,d}$ well. Therefore, it can be concluded that $\alpha'_{S,d}$ provides a good approximation of $\alpha_{S,d}$.

We decompose the random walk for k-RDM as the several independent random walks for 1-RDM. Any two different elements $i, j \in S$ are treated as an independent 1-RDM random walk that starts from $\gamma_i\gamma_j$. After the overall random walk, the probability of $|\gamma_S, \gamma_S\rangle\rangle$ being at a specific site equals the product of the probabilities of each 1-RDM γ'_S at that site. As a result, the sum of probabilities at these specific sites can be expressed as a production $\prod \alpha_{\{i,j\},d}$. We consider the overall random walk as the superposition of all such production

$$\alpha'_{S,d} = c' \sum_{\Lambda\in\text{Par}(S)} \prod_{(i,j)\in\Lambda} \alpha^L_{\{i,j\},d}, \tag{25}$$

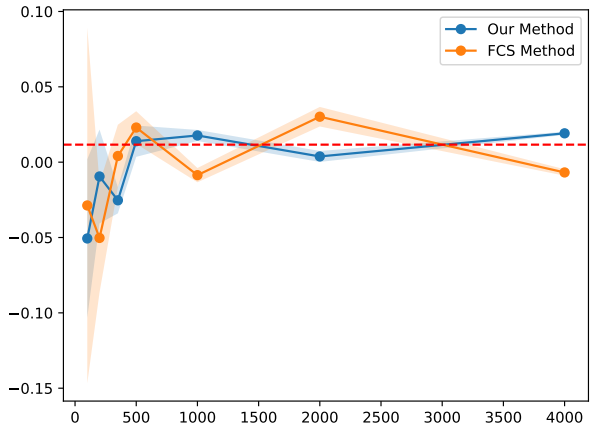

FIG. 4: Caption

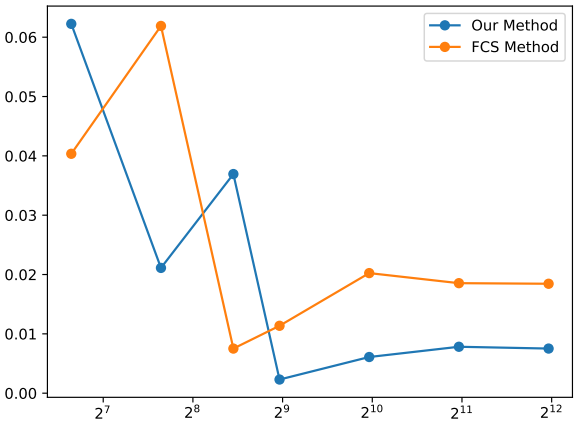

FIG. 5: Caption

where $\mathrm{Par}(S)$ is the set whose elements Λ are sets representing pairwise partitions of S. For example, $S = \{1, 2, 3, 4\}$ and $\Lambda = \{(1, 2), (3, 4)\}$ is a pairwise partitions of S. Similar to Eq. (24), the coefficient c' is selected such that the value of $\alpha'_{S,d}$ at infinite depth matches the value of $\alpha_{S,d}$

$$c' = \frac{n^k}{(2k-1)!!} \frac{\binom{n}{k}}{\binom{2n}{2k}}. \tag{26}$$

We compare the expression $\alpha'_{S,d}$ with true $\alpha_{S,d}$ and show the results in Fig. 3. The curve of $\alpha'_{S,d}$ is very close to the $\alpha_{S,d}$, which suggests that the $\alpha'_{S,d}$ is a good approximation of $\alpha_{S,d}$ as well.

IV. NUMERICAL SIMULATION

In this section, we apply ADFCS to random state ρ to get the expectation of observable γ_S

[1] Alán Aspuru-Guzik, Anthony D Dutoi, Peter J Love, and Martin Head-Gordon. Simulated quantum computation of molecular energies. *Science*, 309(5741):1704–1707, 2005.

[2] Yudong Cao, Jonathan Romero, Jonathan P Olson, Matthias Degroote, Peter D Johnson, Mária Kieferová, Ian D Kivlichan, Tim Menke, Borja Peropadre, Nicolas PD Sawaya, et al. Quantum chemistry in the age of quantum computing. *Chemical reviews*, 119(19):10856–10915, 2019.

[3] Hsin-Yuan Huang, Richard Kueng, and John Preskill. Predicting many properties of a quantum system from very few measurements. *Nature Physics*, 16(10):1050–1057, 2020.

[4] Andrew Zhao, Nicholas C. Rubin, and Akimasa Miyake. Fermionic partial tomography via classical shadows. *Phys. Rev. Lett.*, 127:110504, Sep 2021.

[5] Guang Hao Low. Classical shadows of fermions with particle number symmetry. *arXiv preprint arXiv:2208.08964*, 2022.

[6] Kianna Wan, William J. Huggins, Joonho Lee, and Ryan Babbush. Matchgate shadows for fermionic quantum simulation, 2022.

[7] Ketan N Patel, Igor L Markov, and John P Hayes. Optimal synthesis of linear reversible circuits. *Quantum Inf. Comput.*, 8(3):282–294, 2008.

[8] Jiaqing Jiang, Xiaoming Sun, Shang-Hua Teng, Bujiao Wu, Kewen Wu, and Jialin Zhang. Optimal space-depth trade-off of cnot circuits in quantum logic synthesis. In *Proceedings of the Fourteenth Annual ACM-SIAM Symposium on Discrete Algorithms*, pages 213–229. SIAM, 2020.

[9] Zhang Jiang, Kevin J Sung, Kostyantyn Kechedzhi, Vadim N Smelyanskiy, and Sergio Boixo. Quantum algorithms to simulate many-body physics of correlated fermions. *Physical Review Applied*, 9(4):044036, 2018.

[10] Frank Arute, Kunal Arya, Ryan Babbush, Dave Bacon, Joseph C Bardin, Rami Barends, Rupak Biswas, Sergio Boixo, Fernando GSL Brandao, David A Buell, et al. Quantum supremacy using a programmable superconducting processor. *Nature*, 574(7779):505–510, 2019.

[11] Yulin Wu, Wan-Su Bao, Sirui Cao, Fusheng Chen, Ming-Cheng Chen, Xiawei Chen, Tung-Hsun Chung, Hui Deng, Yajie Du, Daojin Fan, Ming Gong, Cheng Guo, Chu Guo, Shaojun Guo, Lianchen Han, Linyin Hong, He-Liang Huang, Yong-Heng Huo, Liping Li, Na Li, Shaowei Li, Yuan Li, Futian Liang, Chun Lin, Jin Lin, Haoran Qian, Dan Qiao, Hao Rong, Hong Su, Lihua Sun, Liangyuan Wang, Shiyu Wang, Dachao Wu, Yu Xu, Kai Yan, Weifeng Yang, Yang Yang, Yangsen Ye, Jianghan Yin, Chong Ying, Jiale Yu, Chen Zha, Cha Zhang, Haibin Zhang, Kaili Zhang, Yiming Zhang, Han Zhao, Youwei Zhao, Liang Zhou, Qingling Zhu, Chao-Yang Lu, Cheng-Zhi Peng, Xiaobo Zhu, and Jian-Wei Pan. Strong quantum computational advantage using a superconducting quantum processor. *Phys. Rev. Lett.*, 127:180501, Oct 2021.

[12] Sirui Cao, Bujiao Wu, Fusheng Chen, Ming Gong, Yulin Wu, Yangsen Ye, Chen Zha, Haoran Qian, Chong Ying, Shaojun Guo, et al. Generation of genuine entanglement up to 51 superconducting qubits. *Nature*, 619(7971):738–742, 2023.

[13] Christian Bertoni, Jonas Haferkamp, Marcel Hinsche, Marios Ioannou, Jens Eisert, and Hakop Pashayan. Shallow shadows: Expectation estimation using low-depth random clifford circuits. *Physical Review Letters*, 133(2):020602, 2024.

[14] Thomas Schuster, Jonas Haferkamp, and Hsin-Yuan Huang. Random unitaries in extremely low depth. *arXiv preprint arXiv:2407.07754*, 2024.

[15] Pierre-Gabriel Rozon, Ning Bao, and Kartiek Agarwal. Optimal twirling depth for classical shadows in the presence of noise. *Phys. Rev. Lett.*, 133:130803, Sep 2024.

[16] Lucas Hackl and Eugenio Bianchi. Bosonic and fermionic gaussian states from kähler structures. *SciPost Physics Core*, 4(3):025, 2021.

[17] Leslie G. Valiant. Quantum circuits that can be simulated classically in polynomial time. *SIAM Journal on Computing*, 31(4):1229–1254, 2002.

[18] Senrui Chen, Wenjun Yu, Pei Zeng, and Steven T. Flammia. Robust shadow estimation. *PRX Quantum*, 2:030348, Sep 2021.

[19] Ari M. Turner, Frank Pollmann, and Erez Berg. Topological phases of one-dimensional fermions: An entanglement point of view. *Phys. Rev. B*, 83:075102, Feb 2011.

[20] Luca Giuggioli. Exact spatiotemporal dynamics of confined lattice random walks in arbitrary dimensions: a century after smoluchowski and pólya. *Physical Review X*, 10(2):021045, 2020.

[21] Gregory F Lawler and Vlada Limic. *Random walk: a modern introduction*, volume 123. Cambridge University Press, 2010.

Appendix A: Introduction to Pauli-transfer matrix representation

In this work, we focus on the average action of random matchgates. The channel formed by this average action maps a state γ_S to a linear combination of states of the form γ_S. By employing the Jordan-Wigner transformation, we can express γ_S in terms of Pauli operators. The Pauli-transfer matrix (PTM) representation uses these Pauli

operators as a basis, allowing us to write the expectation of ρ in the form:

$$\rho_a = \mathrm{Tr}(\rho\sigma_a)$$

This formulation facilitates subsequent analysis. In the PTM framework, a channel can be represented as:

$$\Lambda_b^a = \mathrm{Tr}(\sigma_b\Lambda(\sigma_a)).$$

Using this expression, we can represent the second moment of the random matchgate as a fourth-order tensor, which is shown in Appendix. B

Appendix B: Majorana operators could diagonalize shadow channel

This section shows the details about diagonalizing shadow channel $\mathcal{M}_d$. Notice that the computational basis $|b\rangle$ are Gaussian states

$$|b\rangle\langle b| = \prod_{j=1}^{n} \frac{1}{2}\left(I - \mathrm{i}(-1)^{b_j}\gamma_{2j-1}\gamma_{2j}\right). \tag{B1}$$

Thus, any basis $|b\rangle\langle b|$ can be prepared from the state $|b\rangle\langle b|$ by a Gaussian unitary $U_Q \in \mathbb{M}_n$, which indicates that Pauli-X is in the matchgate group. The state $|b\rangle = |b_1 b_2 \cdots b_n\rangle$ could be denoted as $\prod X_i^{b_i}|0\rangle$. Since Pauli-X is in the matchgate group, we can absorb the $\prod X_{b_i}$ into the matchgates U_{Q_d} in the expression of shadow channel

$$\mathcal{M}_d(\gamma_S) = \int \mathrm{d}U_{Q_d} \sum_{b\in\{0,1\}^n} \langle b| U_{Q_d}\gamma_S U_{Q_d}^\dagger |b\rangle U_{Q_d}^\dagger |b\rangle \langle b| U_{Q_d} \tag{B2}$$

$$= 2^n \int \mathrm{d}U_{Q_d} \langle 0| U_{Q_d}\gamma_S U_{Q_d}^\dagger |0\rangle U_{Q_d}^\dagger |0\rangle \langle 0| U_{Q_d}. \tag{B3}$$

If S' is not equal to S and the layer number d is not equal to zero, then there exists a permutation matrix Q such that

$$[\gamma_S, U_Q] = 0, \quad \{\gamma_{S'}, U_{Q'}\} = 0. \tag{B4}$$

It implies

$$\frac{1}{2^n}\mathrm{Tr}\left(\gamma_{S'}\mathcal{M}_d(\gamma_S)\right) = \int \mathrm{d}U_{Q_d} \langle 0| U_{Q_d}\gamma_S U_{Q_d}^\dagger |0\rangle \langle 0| U_Q\gamma_{S'} U_{Q_d}^\dagger |0\rangle \tag{B5}$$

$$= \int \mathrm{d}U_{Q_d} \langle 0| U_{Q_d}U_{Q'_d}\gamma_S U_{Q'_d}^\dagger U_{Q_d}^\dagger |0\rangle \langle 0| U_{Q_d}U_{Q'_d}\gamma_{S'} U_{Q'_d}^\dagger U_{Q_d}^\dagger |0\rangle \tag{B6}$$

$$= -\int \mathrm{d}U_{Q_d} \langle 0| U_{Q_d}\gamma_S U_{Q_d}^\dagger |0\rangle \langle 0| U_{Q_d}\gamma_{S'} U_{Q_d}^\dagger |0\rangle. \tag{B7}$$

The result shows that $\mathrm{Tr}\left(\gamma_{S'}\mathcal{M}_d(\gamma_S)\right) = 0$ when S' is not equal to S, thereby $\mathcal{M}_d(\gamma_S) = \alpha_{s,d}\gamma_S$.

Appendix C: Bound the variance of ADFCS estimator

Proof. Let the estimator of the observable γ_S be v.

$$\mathrm{Var}[v] \leq \mathbb{E}[|v|^2] \tag{C1}$$

$$= \int \mathrm{d}U_{Q_d} \mathop{\mathbb{E}}_{\rho} \left[\sum_b \langle b| U_{Q_d} \rho U_{Q_d}^\dagger |b\rangle \left| \langle b| U_{Q_d} \mathcal{M}_d^{-1}(\gamma_S) U_{Q_d}^\dagger |b\rangle \right|^2 \right] \tag{C2}$$

$$= 2^{-n} \int \mathrm{d}U_{Q_d} \sum_b \left| \langle b| U_{Q_d} \mathcal{M}_d^{-1}(\gamma_S) U_{Q_d}^\dagger |b\rangle \right|^2 \tag{C3}$$

$$= \frac{1}{|\alpha_{S,d}|^2} \int \langle 0| U_{Q_d} \gamma_S U_{Q_d}^\dagger |0\rangle \langle 0| U_{Q_d} \gamma_S^\dagger U_{Q_d}^\dagger |0\rangle \tag{C4}$$

$$= \frac{1}{\alpha_{S,d}}. \tag{C5}$$

Appendix D: Details of simplifying $\alpha_{S,d}$ to tensore network.

In this section, we represent the variance of Fermionic classical shadow in the form of a tensor network. The variance is bounded by $1/\alpha_{S,d}$, where

$$\alpha_{S,d} = \int_{Q\sim O_d} \mathrm{d}\mu(Q) \left| \langle 0| U_Q \gamma_S U_Q^\dagger |0\rangle \right|^2 \tag{D1}$$

$$= \int_{Q\sim O_d} \mathrm{d}\mu(Q) \langle 0| U_Q \gamma_S U_Q^\dagger |0\rangle \langle 0| U_Q \gamma_S^\dagger U_Q^\dagger |0\rangle . \tag{D2}$$

The subscript d denotes the layer number of the matchgate circuit. The expression could be simplified by substituting the relationship between $\gamma_S^\dagger$ and γ_S, which is

$$\gamma_S^\dagger = (-1)^{\frac{|S|(|S|-1)}{2}} \gamma_S. \tag{D3}$$

The relation is true because of the anti-commutation relation of Majorana operators $\{\gamma_i, \gamma_j\} = 2\delta_{ij}$. The anti-commutation relation produces a coefficient of $(-1)^{|S|-1}$ when γ_{l_1} is moved to the first place. Then, the $\gamma_S^\dagger$ could be calculated by

$$\gamma_S^\dagger = (-1)^{|S|-1} \gamma_{l_1} \gamma_{l_{|S|}} \gamma_{l_{|S|-1}} \cdots \gamma_{l_2} \tag{D4}$$

$$= (-1)^{|S|-1+|S|-2} \gamma_{l_1} \gamma_{l_2} \gamma_{l_{|S|}} \gamma_{l_{|S|-1}} \cdots \gamma_{l_3} \tag{D5}$$

$$= (-1)^{\frac{|S|(|S|-1)}{2}} \gamma_S. \tag{D6}$$

By substituting Eq. (D6), the $\alpha_{S,d}$ could be expressed as

$$\alpha_{S,d} = (-1)^{\frac{|S|(|S|-1)}{2}} \int_{Q\sim O_d} \mathrm{d}\mu(Q) \langle 0| U_Q \gamma_S U_Q^\dagger |0\rangle^2 \tag{D7}$$

$$= (-1)^{\frac{|S|(|S|-1)}{2}} \int_{Q\sim O_d} \mathrm{d}\mu(Q) \,\mathrm{tr}\Big(U_Q \gamma_S U_Q^\dagger |0\rangle \langle 0| \Big)^2 \tag{D8}$$

$$= (-1)^{\frac{|S|(|S|-1)}{2}} 2^{2n} \int_{Q\sim O_d} \mathrm{d}\mu(Q) \langle\langle 0,0| \mathcal{U}_Q \otimes \mathcal{U}_Q |\gamma_S, \gamma_S\rangle\rangle \tag{D9}$$

$$= (-1)^{\frac{|S|(|S|-1)}{2}} 2^{2n} \langle\langle 0,0| \int_{Q\sim O_d} \mathrm{d}\mu(Q) \mathcal{U}_Q^{\otimes 2} |\gamma_S, \gamma_S\rangle\rangle. \tag{D10}$$

In the third line, we rewrite the formula regarding super vectors and super operators. The integral of the form $\int \mathrm{d}\mu(Q) \mathcal{U}_Q^{\otimes k}$ is known as the twirling. Sometimes we will use the terminology *twirling* for simplification.

The d-layer matchgate circuit is composed of interweaving stacking two-qubits matchgates. Thus, to calculate the integral $\int_{Q\sim O_d} \mathrm{d}\mu(Q) \mathcal{U}_Q^{\otimes 2}$, we could independently calculate the integral of each 2 qubits matchgates. The result of

the integral of the 2 qubits matchgates is given by Lemma 2

$$\int_{Q\sim M_2} \mathrm{d}\mu(Q)\mathcal{U}_Q^{\otimes 2} = |\gamma_\emptyset\rangle\rangle|\gamma_\emptyset\rangle\rangle\langle\langle\gamma_\emptyset|\langle\langle\gamma_\emptyset| + \frac{1}{4}\sum_{i,j}|\gamma_i\rangle\rangle|\gamma_i\rangle\rangle\langle\langle\gamma_j|\langle\langle\gamma_j| \tag{D11}$$

$$+\frac{1}{6}\sum_{\substack{i_1\neq i_2\\ j_1\neq j_2}}|\gamma_{i_1}\gamma_{i_2}\rangle\rangle|\gamma_{i_1}\gamma_{i_2}\rangle\rangle\langle\langle\gamma_{j_1}\gamma_{j_2}|\langle\langle\gamma_{j_1}\gamma_{j_2}| \tag{D12}$$

$$+\frac{1}{4}\sum_{\substack{i_1\neq i_2, j_1\neq j_2\\ i_1\neq i_3, j_1\neq j_3\\ i_2\neq i_3, j_2\neq j_3}}|\gamma_{i_1}\gamma_{i_2}\gamma_{i_3}\rangle\rangle|\gamma_{i_1}\gamma_{i_2}\gamma_{i_3}\rangle\rangle\langle\langle\gamma_{j_1}\gamma_{j_2}\gamma_{j_3}|\langle\langle\gamma_{j_1}\gamma_{j_2}\gamma_{j_3}| \tag{D13}$$

$$+|\gamma_1\gamma_2\gamma_3\gamma_4\rangle\rangle|\gamma_1\gamma_2\gamma_3\gamma_4\rangle\rangle\langle\langle\gamma_1\gamma_2\gamma_3\gamma_4|\langle\langle\gamma_1\gamma_2\gamma_3\gamma_4|, \tag{D14}$$

where i, j are index ranged from 1 to 4.

To calculate the interweaving stacking of two-qubits matchgates, we represent the super vectors $|\gamma_S\rangle\rangle$ using the Pauli basis through the Jordan-Wigner transformation. Due to the transformation, the γ_S is corresponded to a Pauli basis with a phase $\pm \mathrm{i}^{\lfloor |S|/2 \rfloor}$. Thus, the super vector $|\gamma_S, \gamma_S\rangle\rangle$ could be represented as

$$|\gamma_S, \gamma_S\rangle\rangle = (-1)^{\lfloor \frac{|S|}{2} \rfloor}|P^S, P^S\rangle\rangle, \tag{D15}$$

where P^S is the Pauli operator that corresponding to the γ_S. Therefore, due to the Lemma 3, the net phase of the $\alpha_{S,d}$ is 1.

We also represent the integral of the 2 qubits matchgates with Pauli basis by applying the Jordan-Wigner transformation to Eq. (D11). Denote the twirling as a 4-bond tensor as the following rule,

$$T^{\sigma_1,\sigma_2}_{\sigma_3,\sigma_4} = \langle\langle\sigma_1,\sigma_2|\langle\langle\sigma_1,\sigma_2|\int_{Q\sim M_2}\mathrm{d}\mu(Q)\mathcal{U}_Q^{\otimes 2}|\sigma_3,\sigma_4\rangle\rangle|\sigma_3,\sigma_4\rangle\rangle, \tag{D16}$$

where $\sigma_1, \sigma_2, \sigma_3, \sigma_4$ are two-qubits Pauli operators. The concrete elements of the tensor T is shown in the Table I. For example, due to Eq. (D11) and Eq. (D16), T^{XY}_{YZ} is equal to $\frac{1}{6}$.

To build the tensor network, we will define some notation. Let $T^{(o)}$ represent the odd-layer of T gates, and $T^{(e)}$ represent the even-layer of T gates, which are shown in the following circuits.

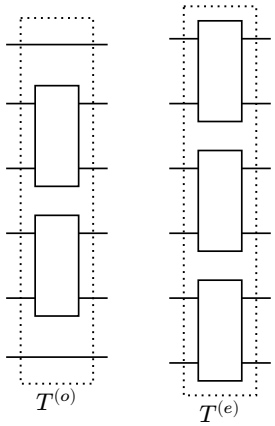

The whole tensor network $T^{(\mathrm{whole})}$ could be expressed by alternately apply $T^{(o)}$ and $T^{(e)}$ gates,

$$T^{(\mathrm{whole})}(t, b_1, b_2) = {T^{(o)}}^{b_2}\left(\prod_{i=0}^{t} T^{(e)}T^{(o)}\right){T^{(e)}}^{b_1}, \tag{D17}$$

where $b_1, b_2 \in \{0, 1\}$, $t + b_1 + b_2$ stands for the number of layers.

The calculation of $\alpha_{S,d}$ could be represented by the tensor network contraction. Notice the matrix identity

$$|0\rangle\langle 0| = \frac{1}{2^n}\sum_{\Lambda\subset[2n]}\prod_{i\in\Lambda} Z_i, \tag{D18}$$

where Z_i denotes the application of the Pauli Z operator to the i-th qubit. Specially, let $\prod_{i\in\emptyset} Z_i = \mathbb{I}_n$. Then, the super vector of $|0,0\rangle\rangle$ could be expressed as

$$|0,0\rangle\rangle = \frac{1}{2^{2n}}\sum_{\Lambda,\Lambda'\subset[2n]} |\prod_{i\in\Lambda} Z_i, \prod_{j\in\Lambda'} Z_j\rangle\rangle. \tag{D19}$$

By transforming all the super vectors and the super operators in the Pauli basis, the evolution of $\mathcal{U}_Q|\gamma_S\rangle\rangle$ could be equivalently expressed by

$$\int \mathrm{d}\mu(Q)\mathcal{U}_Q^{\otimes 2}|\gamma_S,\gamma_S\rangle\rangle = T^{(\mathrm{whole})}|P^S\rangle\rangle. \tag{D20}$$

In the equation, for simplicity, we slightly abuse the notation $|P^S\rangle\rangle$ to represent the tensor of Pauli basis $|P^S,P^S\rangle\rangle$. Formally, $|P^S\rangle\rangle$ is the tensor δ_S^R, where $\delta_S^R = 1$ if and only if $R = S$, otherwise, $\delta_S^R = 0$. In this representation, The tensor contraction $T^{(\mathrm{whole})}(t,b_1,b_2)P^S$ is equivalent to the evolution $\int \mathrm{d}\mu(Q)\mathcal{U}_Q^{\otimes 2}|\gamma_S,\gamma_S\rangle\rangle$. Thus, the calculation of $\alpha_{S,d}$ could be expressed as the tensor network contraction, as illustrated in Fig. 2. polish the figure

Lemma 2 (Theorem 1 in [6])**.** *Let Q be a matrix uniformly randomly sampled from orthogonal group $\mathcal{O}(n)$, then*

$$\int_{Q\sim\mathbb{M}_n} \mathrm{d}\mu(Q)\mathcal{U}_Q = |\mathbb{I}\rangle\rangle\langle\langle\mathbb{I}| \tag{D21}$$

$$\int_{Q\sim\mathbb{M}_n} \mathrm{d}\mu(Q)\mathcal{U}_Q^{\otimes 2} = \sum_{k=0}^{2n} |\mathcal{R}_k^{(2)}\rangle\rangle\langle\langle\mathcal{R}_k^{(2)}| \tag{D22}$$

$$\int_{Q\sim\mathbb{M}_n} \mathrm{d}\mu(Q)\mathcal{U}_Q^{\otimes 3} = \sum_{\substack{k_1,k_2,k_3\geq 0\\ k_1+k_2+k_3\leq 2n}} |\mathcal{R}_{k_1,k_2,k_3}^{(3)}\rangle\rangle\langle\langle\mathcal{R}_{k_1,k_2,k_3}^{(3)}|. \tag{D23}$$

where

$$|\mathcal{R}_k^{(2)}\rangle\rangle = \binom{2n}{k}^{-1/2}\sum_{S\subseteq[2n],|S|=k} |\gamma_S\rangle\rangle|\gamma_S\rangle\rangle \tag{D24}$$

$$|\mathcal{R}_k^{(3)}\rangle\rangle = \binom{2n}{k_1,k_2,k_3,2n-k_1-k_2-k_3}^{-1/2}\sum_{\substack{S_1,S_2,S_3\subseteq[2n] disjoint\\ |S_j|=k_j,1\leq j\leq 3}} |\gamma_{S_1}\gamma_{S_2}\rangle\rangle|\gamma_{S_2}\gamma_{S_3}\rangle\rangle|\gamma_{S_3}\gamma_{S_1}\rangle\rangle \tag{D25}$$

Lemma 3. *The net phase of $\alpha_{S,d}$ is* 1.

Proof. The net phase of $\alpha_{S,d}$ is 1 is $(-1)^{\frac{|S|(|S|-1)}{2}}(-1)^{\lfloor|S|/2\rfloor}$. We categorize the discussion of the parity of $|S|$.

1. $|S|$ **is an odd number.** Let $|S| = 2q+1$, $q\in\mathbb{N}$, $q\geq 0$. And then

$$(-1)^{\frac{|S|(|S|-1)}{2}}(-1)^{\lfloor|S|/2\rfloor} = (-1)^{q(2q+1)+q} = 1. \tag{D26}$$

2. $|S|$ **is an even number.** Let $|S| = 2q$, $q\in\mathbb{N}$, $q\geq 0$. And then

$$(-1)^{\frac{|S|(|S|-1)}{2}}(-1)^{\lfloor|S|/2\rfloor} = (-1)^{(2q-1)q+q} = 1. \tag{D27}$$

□

□

T	II	IX	IY	IZ	XI	XX	XY	XZ	YI	YX	YY	YZ	ZI	ZX	ZY	ZZ
II	1															
IX		1/4	1/4					1/4				1/4				
IY		1/4	1/4					1/4				1/4				
IZ				1/6		1/6	1/6			1/6	1/6		1/6			
XI					1/4				1/4					1/4	1/4	
XX				1/6		1/6	1/6			1/6	1/6		1/6			
XY				1/6		1/6	1/6			1/6	1/6		1/6			
XZ		1/4	1/4					1/4				1/4				
YI					1/4				1/4					1/4	1/4	
YX				1/6		1/6	1/6			1/6	1/6		1/6			
YY				1/6		1/6	1/6			1/6	1/6		1/6			
YZ		1/4	1/4					1/4				1/4				
ZI				1/6		1/6	1/6			1/6	1/6		1/6			
ZX					1/4				1/4					1/4	1/4	
ZY					1/4				1/4					1/4	1/4	
ZZ																1

TABLE I: Values of tensor T. The head of columns represents the input of T while the head of rows represents the output of T. For example, the value in row 'XY' and column 'YZ' represent the value T^{XY}_{YZ}. The blank space of the table stands for 0.

$$\begin{array}{ccccccc}
\mathrm{span}\{\gamma_i\gamma_j\} & \longrightarrow & V_P & \longrightarrow & \mathcal{P}_n & \longrightarrow & \mathcal{P}_N \\
\Big\downarrow T^{(\mathrm{whole})} & & \Big\downarrow T^{(\mathrm{whole})}_{V_P} & & \Big\downarrow T^{(\mathrm{whole})}_{\mathcal{P}_n} & & \Big\downarrow T^{(\mathrm{whole})}_{\mathcal{P}_N} \\
\mathrm{span}\{\gamma_i\gamma_j\} & \longrightarrow & V_P & \longrightarrow & \mathcal{P}_n & \longrightarrow & \mathcal{P}_N
\end{array}$$

FIG. 6: The diagram shows how we simplify the calculation step by step. The horizontal arrows point from a high-dimensional space to a relatively low-dimensional space. The vertical arrows stand for the corresponding operators of $T^{(\mathrm{whole})}(t, b_1, b_2)$ in different representations. Finally, we reduce it to the N-elementary polynomial of the 2nd degree polynomial space.

Appendix E: Mapping the action of tensors to random walk

1. Reduce the calculation to polynomial space

We represent $T^{(\mathrm{whole})}$ using polynomial space because it provides the essential properties we require, such as multiplication and addition, which will be important for our later work.

Notice that the space V_P is isometric to the n-elementary polynomial of the 2nd degree polynomial space $\mathcal{P}_n$. The isometric could be constructed by the following

$$\begin{aligned} \phi : V_P &\to \mathcal{P}_n \\ |M_i(\prod Z_k)M_j\rangle\rangle &\mapsto x_i x_j \\ |Z_i\rangle\rangle &\mapsto x_i^2. \end{aligned} \tag{E1}$$

The linear map ϕ is a homomorphism with inverse, which means it is an isometric between V_P and $\mathcal{P}_n$. The equivalent representation of $T^{(\mathrm{whole})}$ could be constructed by

$$T^{(\mathrm{whole})}_{\mathcal{P}_n}(t)(\cdot) := \phi \circ T^{(\mathrm{whole})}(t, 1, 0) \circ \phi^{-1}(\cdot). \tag{E2}$$

We could also transfer the input of $T^{(\text{whole})}$ to space $\mathcal{P}_n$,

$$\gamma_{ij} \longrightarrow |M_i(\prod Z_k)M_j\rangle\rangle \xrightarrow{\phi} x_i x_j. \tag{E3}$$

Thus, the action of d-layer matchgate circuit on the γ_{ij} is equivalent to the action of $T^{(\text{whole})}_{\mathcal{P}_n}(t)$ on the term $x_i x_j$. Due to Lemma 4, the action could be further simplified by finding a sub-representation $\mathcal{P}_N$ of representation $\mathcal{P}_n$, where N equals to $\frac{n}{2}$. Recall that n is an even number so N is an integer.

Certain hidden patterns are revealed by reducing the representation to the polynomial space $\mathcal{P}_N$. Most of the main results are been proved in the $\mathcal{P}_N$.

Lemma 4. *The space $\mathcal{P}_N$ isometric to a sub-representation of $\mathcal{P}_n$.*

Proof. Define the map ϕ as

$$\begin{aligned} \phi : \mathcal{P}_N &\to \mathcal{P}_n \\ y_i^2 &\mapsto x_{2i-1}^2 + 4x_{2i-1}x_{2i} + x_{2i}^2 \\ y_i y_j &\mapsto (x_{2i-1} + x_{2i})(x_{2j-1} + x_{2j}). \end{aligned} \tag{E4}$$

We define the ϕ as a linear function so that the definition of mapping on a basis induces the mapping on any element of the space

$$\phi(\sum \xi_{ij} y_i y_j) = \sum \xi_{ij} \phi(y_i y_j). \tag{E5}$$

Thus, the space $\phi(\mathcal{P}_N)$ is a linear subspace of $\mathcal{P}_n$. Because ϕ is an injection, there is a map $\phi' : \mathcal{P}_n \to \mathcal{P}_N$ such that $\phi' \circ \phi$ is identity. Define the group action $T^{(\text{whole})}_{\mathcal{P}_N}$ as

$$T^{(\text{whole})}_{\mathcal{P}_N}(y_i y_j) := \phi' \circ T^{(\text{whole})}_{\mathcal{P}_n} \circ \phi(y_i y_j). \tag{E6}$$

Based on the definition of representation, we know that the space $\mathcal{P}_N$ with the group action $T^{(\text{whole})}_{\mathcal{P}_N}$ is a representation.

The next step is to show that such a representation $T^{(\text{whole})}_{\mathcal{P}_N}$ does not lose information. Formally, we need to prove that the representation $\mathcal{P}_n$ could be reduced to a sub-representation isometrics to $\mathcal{P}_N$. Naturally, we will consider whether the subspace $\phi(\mathcal{P}_N)$ will constitute a sub-representation. If it is true, the proof is done because $\phi(\mathcal{P}_N) \simeq \mathcal{P}_N$.

By the definition of sub-representation, we need to prove

$$T^{(\text{whole})}_{\mathcal{P}_n}(t)(\phi(\mathcal{P}_N)) \subset \phi(\mathcal{P}_N), \quad \forall t. \tag{E7}$$

The readers may recall that the formal representation is $T^{(e)}_{\mathcal{P}_n}\phi(\mathcal{P}_N)$ rather than $\phi(\mathcal{P}_N)$. Here, we remove the ambiguity by proving $T^{(e)}_{\mathcal{P}_n}\phi(\mathcal{P}_N) = \phi(\mathcal{P}_N)$. By expanding the definition of $T^{(e)}_{\mathcal{P}_n}$, we could get the calculation of $T^{(e)}_{\mathcal{P}_n}\phi(y_i y_j)$ backs to the space V_P. Then, we will find that $T^{(e)}_{\mathcal{P}_n}\phi(y_i y_j) = \phi(y_i y_j)$ from the Table I. Thus, we have $T^{(e)}_{\mathcal{P}_n}\phi(\mathcal{P}_N) = \phi(\mathcal{P}_N)$.

The statement (E7) will be proved by induction.

When $t = 0$, $T^{(e)}_{\mathcal{P}_n}\phi(\mathcal{P}_N) \subset \phi(\mathcal{P}_N)$ is true. Suppose the statement is true for t^*, then we have

$$T^{(\text{whole})}_{\mathcal{P}_n}(t^*)(\phi(y_i y_j)) = \sum \xi_{lm} \phi(y_l y_m). \tag{E8}$$

And then

$$T^{(\text{whole})}_{\mathcal{P}_n}(t^*+1)(\phi(y_i y_j)) = T^{(e)}_{\mathcal{P}_n} T^{(o)}_{\mathcal{P}_n}(\sum \xi_{lm}\phi(y_l y_m)) \tag{E9}$$

$$= \sum \xi_{lm}\delta_{lm} T^{(e)}_{\mathcal{P}_n} T^{(o)}_{\mathcal{P}_n}(x_{2i-1}^2 + 4x_{2i-1}x_{2i} + x_{2i}^2) \tag{E10}$$

$$+ \sum \xi_{lm}(1-\delta_{lm}) T^{(e)}_{\mathcal{P}_n} T^{(o)}_{\mathcal{P}_n}\left((x_{2i-1} + x_{2i})(x_{2j-1} + x_{2j})\right) \tag{E11}$$

We will prove Eq. (E10) is in the space $\phi(\mathcal{P}_N)$, while the same result of Eq. (E11) can be proved by the same method.

Now, we will directly calculate this expression

$$
\begin{aligned}
&T^{(e)}_{\mathcal{P}_n}T^{(o)}_{\mathcal{P}_n}(x^2_{2i-1}+4x_{2i-1}x_{2i}+x^2_{2i})\\
=&T^{(e)}_{\mathcal{P}_n}(\frac{1}{6}x^2_{2i-2}+\frac{2}{3}x_{2i-2}x_{2i-1}+x_{2i-2}x_{2i}+x_{2i-2}x_{2i+1}\\
&+\frac{1}{6}x^2_{2i-1}+x_{2i-1}x_{2i}+x_{2i-1}x_{2i+1}\\
&+\frac{1}{6}x^2_{2i}+\frac{2}{3}x_{2i}x_{2i+1}+\frac{1}{6}x^2_{2i+1})\\
=&\frac{1}{36}x^2_{2i-3}+\frac{1}{9}x_{2i-3}x_{2i-2}+\frac{5}{12}x_{2i-3}x_{2i-1}+\frac{5}{12}x_{2i-3}x_{2i}+\frac{1}{4}x_{2i-3}x_{2i+1}+\frac{1}{4}x_{2i-3}x_{2i+2}\\
&+\frac{1}{36}x^2_{2i-2}+\frac{5}{12}x_{2i-2}x_{2i-1}+\frac{5}{12}x_{2i-2}x_{2i}+\frac{1}{4}x_{2i-2}x_{2i+1}+\frac{1}{4}x_{2i-2}x_{2i+2}\\
&+\frac{2}{9}x^2_{2i-1}+\frac{8}{9}x_{2i-1}x_{2i}+\frac{5}{12}x_{2i-1}x_{2i+1}+\frac{5}{12}x_{2i-1}x_{2i+2}\\
&+\frac{2}{9}x^2_{2i}+\frac{5}{12}x_{2i}x_{2i+1}+\frac{5}{12}x_{2i}x_{2i+2}\\
&+\frac{1}{36}x^2_{2i+1}+\frac{1}{9}x_{2i+1}x_{2i+2}\\
&+\frac{1}{36}x^2_{2i+2}
\end{aligned}
\tag{E12}
$$

The result expression is in $\phi(\mathcal{P}_N)$ because we could find a polynomial y in $\mathcal{P}_N$ such that $\phi(y)$ equals the result expression,

$$
y=\frac{1}{6}y^2_{i-1}+\frac{5}{3}y_{i-1}y_i+y_{i-1}y_{i+1}+\frac{4}{3}y^2_i+\frac{5}{3}y_{i-1}y_{i+1}+\frac{1}{6}y^2_{i+1} \tag{E13}
$$

$$
\phi(y)=T^{(e)}_{\mathcal{P}_n}T^{(o)}_{\mathcal{P}_n}(x^2_{2i-1}+4x_{2i-1}x_{2i}+x^2_{2i}) \tag{E14}
$$

Thus, we get that

$$
T^{(e)}_{\mathcal{P}_n}T^{(o)}_{\mathcal{P}_n}(x^2_{2i-1}+4x_{2i-1}x_{2i}+x^2_{2i})\subset\phi(\mathcal{P}_N). \tag{E15}
$$

Thus, Eq. (E12) is contained in the space $\phi(\mathcal{P}_N)$, which completes the proof. □

2. Mapping the spread of polynomials to random walk

The action of layers is the lazy-symmetry random walk on a 2D square lattice in most sites. To illustrate this point, we will begin with a specific example. Considering $1<i<N-1$ and $i+1<j\leq N$, the action of $T^{(e)}_{\mathcal{P}_N}T^{(o)}_{\mathcal{P}_N}$ is

$$
T^{(e)}_{\mathcal{P}_N}T^{(o)}_{\mathcal{P}_N}(y_iy_j)=\left(\frac{1}{4}y_{i-1}+\frac{1}{2}y_i+\frac{1}{4}y_{i-1}\right)\left(\frac{1}{4}y_{j-1}+\frac{1}{2}y_j+\frac{1}{4}y_{j-1}\right). \tag{E16}
$$

In this case, the action of $T^{(e)}_{\mathcal{P}_N}T^{(o)}_{\mathcal{P}_N}$ can be viewed as first independently evolving y_i and y_j in a one-dimensional lattice, and then combining them,

$$
\begin{aligned}
y_i&\to\frac{1}{4}y_{i-1}+\frac{1}{2}y_i+\frac{1}{4}y_{i-1}\\
y_j&\to\frac{1}{4}y_{j-1}+\frac{1}{2}y_j+\frac{1}{4}y_{j-1}.
\end{aligned}
\tag{E17}
$$

We observe that this pattern appears in most sites y_iy_j. Therefore, we can analyze the evolving behavior separately in one-dimensional polynomial space (one-dimensional lattice). Afterward, we can examine the differences between the true evolved polynomial and the combined polynomial. This approach is the skeleton of estimating the order of tensor contraction. Now, we will make the above concepts more specific and more concrete.

We introduce the lazy-symmetry random walk in polynomial space, or the one-dimensional lattice, to describe the separate evolution behavior. A lazy-symmetry random walk is a type of Markov process, which is shown in Fig. **??**.

In this process, consider a point located at a site y_i. In the next time interval, this point has a probability of 0.25 moving to one of its neighboring sites y_{i-1} or y_{i+1}, and it has a probability of 0.5 staying in place. If the origin site is on the ends of the lattice, it has a probability of 0.75 staying in place and has a probability of 0.25 moving around. The probability transition relation could be expressed by

$$L\left(y_i\right)=\begin{cases}\frac{3}{4}y_1+\frac{1}{4}y_2, & i=1\\ \frac{1}{4}y_{i-1}+\frac{1}{2}y_i+\frac{1}{4}y_{i+1}, & 1<i<N\\ \frac{3}{4}y_N+\frac{1}{4}y_{N-1}, & i=N.\end{cases} \tag{E18}$$

We could see that the separate evolution in Eq. (E17) fits the form of lazy-symmetry random walk.

In Eq. (E16), we showed the result of how y_iy_j transfers in one specific situation. Now, we will show all possible results in any situation in Table **??**. The table lists all the possible transition results no matter what inputs it receives. It was created in a similar way to the previous example in Eq. (E12).

In Table **??**, we can see that in most cases

$$T^{(e)}_{\mathcal{P}_N}T^{(o)}_{\mathcal{P}_N}(y_iy_j)=L(y_i)L(y_j) \tag{E19}$$

except for the cases when $|i-j|\leq 1$. Moreover, the coefficients of remainder terms $T^{(e)}_{\mathcal{P}_N}T^{(o)}_{\mathcal{P}_N}(y_iy_j)-L(y_i)L(y_j)$ are small. Refs. [20] gives the analytical solution of lazy-symmetry random walk,

$$L^t(y_i)=\sum_{\mu}\mathcal{L}_i(\mu,t)y_\mu, \tag{E20}$$

where $L^t(y_i)$ represents the outcome of random walking t steps from y_i according to the propagation rule L in Eq. (E18), and the $\mathcal{L}_i(\mu,t)$ represents the probability of stopping at y_μ after t-steps random walking,

$$\mathcal{L}_i(\mu,t)=\frac{1}{N}+\frac{2}{N}\sum_{k=1}^{N-1}\cos\left(\left(\mu-\frac{1}{2}\right)\frac{\pi k}{N}\right)\cos\left(\left(i-\frac{1}{2}\right)\frac{\pi k}{N}\right)\cos^{2t}\left(\frac{\pi k}{2N}\right). \tag{E21}$$

Thus, for the evolution that could be separated by $T^{(e)}_{\mathcal{P}_N}T^{(o)}_{\mathcal{P}_N}(y_iy_j)=L(y_i)L(y_j)$, we could get the analytical solution results

$$\begin{aligned}T^{(\text{whole})}_{\mathcal{P}_N}(t)(y_iy_j)=&(T^{(e)}_{\mathcal{P}_N}T^{(o)}_{\mathcal{P}_N})^t(y_iy_j) &\text{(E22)}\\ =&L^t(y_i)L^t(y_j)+R(y_iy_j) &\text{(E23)}\\ =&\sum_{\mu,\nu}\left(\mathscr{L}_{ij}(\mu,\nu,t)y_\mu y_\nu+\mathscr{R}_{ij}(\mu,\nu,t)y_\mu y_\nu\right), &\text{(E24)}\end{aligned}$$

where

$$\mathscr{L}_{ij}(\mu,\nu,t):=\mathcal{L}_i(\mu,t)\mathcal{L}_j(\nu,t). \tag{E25}$$

The R stands for the remind terms caused by the near-diagonal terms y_iy_j, $|i-j|\leq 1$ in Table **??**.

The calculation of α could be separated into two parts. The first part is contributed by the lazy-symmetry random walk, and the second part is contributed by the remind terms. Recall that the $\alpha_{S,d}$ can be calculated by the tensor contraction of $T^{(\text{whole})}$, $|P^S\rangle\rangle$ and $|0,0\rangle\rangle$. We have mapped the $T^{(\text{whole})}$ and $|P^S\rangle\rangle$ into polynomial space. And the $|0,0\rangle\rangle$ mapped into the polynomial space as well. Eq. (D19) has transformed $|0,0\rangle\rangle$ into Pauli basis. Notice that $\langle\langle Z_i|$ is a linear function which takes a super vector to a number. Especially, it takes $|Z_i\rangle\rangle$ to 1 and takes the other Pauli basis to 0. As we known, the $|Z_i\rangle\rangle$ is mapped to x_i^2 in $\mathcal{P}_n$. The derivative operators $\frac{\partial^2}{\partial x_i^2}$ satisfy all these properties. In another word, The space of derivative operators is the dual space of polynomial space. Thus, we find the mapping from $|Z_i\rangle\rangle$ to $\mathcal{P}_n$

$$|Z_i\rangle\rangle\to\frac{\partial^2}{\partial x_i^2}. \tag{E26}$$

After some algebras, we map the $|0,0\rangle\rangle$ to $\mathcal{P}_N$ when $|S|=2$

$$|0,0\rangle\rangle\to\frac{1}{2^{2n}}\frac{1}{3}\sum_{i,j}\frac{\partial^2}{\partial y_i^2}. \tag{E27}$$

Thus, the $\alpha_{S,2t+1}$ could be expressed as

$$\alpha_{\{\gamma_i\gamma_j\},2t+1} = \frac{1}{3}\sum_{\mu}\frac{\partial^2}{\partial y_\mu^2}T^{(\text{whole})}_{\mathcal{P}_N}(t)(y_i y_j). \tag{E28}$$

Then, we could calculate $\alpha_{S,d}$ in $\mathcal{P}_N$ via combining Eq. (E24)

$$\begin{aligned}\alpha_{\{\gamma_i\gamma_j\},2t+1} =& \frac{1}{3}\sum_{\mu}\mathscr{L}_{ij}(\mu,\mu,t) + \frac{1}{3}\sum_{\mu}\mathscr{R}_{ij}(\mu,\mu,t) &\text{(E29)}\\ =:& \alpha^{\mathscr{L}}_{\{\gamma_i\gamma_j\},2t+1} + \alpha^{\mathscr{R}}_{\{\gamma_i\gamma_j\},2t+1}. &\text{(E30)}\end{aligned}$$

Appendix F: Estimate the order of $\alpha^{\mathscr{L}}_{\{\gamma_i\gamma_j\},2t+1}$

We have separated the calculation of $\alpha_{\{\gamma_i\gamma_j\},2t+1}$ into two parts in Sec. E 2. In this section, we aim to estimate the order of the first part, $\alpha^{\mathscr{L}}_{\{\gamma_i\gamma_j\},2t+1}$.

Theorem 1. *Given $t = o(n^2)$, the $\alpha^{\mathscr{L}}_{\{\gamma_i\gamma_j\},2t+1}$ could be estimated by the following formula*

$$3\alpha^{\mathscr{L}}_{\{\gamma_i\gamma_j\},2t+1} = \frac{1}{\sqrt{2\pi t}}(e^{-\frac{a^2}{2t}} + e^{-\frac{b^2}{2t}}) + \frac{2}{\sqrt{2\pi t}}(e^{-\frac{a^2+n(n/2-a)}{2t}} + e^{-\frac{b^2+n(n/2-b)}{2t}}) + \mathcal{O}\left(e^{-\frac{\pi^2}{2}t}\right), \tag{F1}$$

where a is defined as $|i-j|$ and b is defined as $i+j-1$.

Proof. Recall that $N = n/2$. By Lemma 5, we could simplify the expression of $\alpha^{\mathscr{L}}_{\{\gamma_i\gamma_j\},2t+1}$ into Eq. (F7). Then, we absorb the $k=0$ into the summation

$$\begin{aligned}3\alpha^{\mathscr{L}}_{\{\gamma_i\gamma_j\},2t+1} &= \frac{1}{N} + \frac{1}{N}\sum_{k=1}^{N-1}\left[\cos\left((i-j)\frac{k\pi}{N}\right) + \cos\left((i+j-1)\frac{k\pi}{N}\right)\right]\cos^{4t}\left(\frac{\pi k}{2N}\right)\\ &= -\frac{1}{N} + \frac{1}{N}\sum_{k=0}^{N-1}\left[\cos\left((i-j)\frac{k\pi}{N}\right) + \cos\left((i+j-1)\frac{k\pi}{N}\right)\right]\cos^{4t}\left(\frac{\pi k}{2N}\right).\end{aligned} \tag{F2}$$

In this way, the summation over k will go through a complete cycle/period. This will allow us to utilize some useful properties regarding trigonometric summations.

We want to express this summation as a better-handled integral for computation and analysis purposes. To achieve this, we need to take the following two steps. First, we find that directly turning this into an integral is still not easy to calculate, so we need to replace the term $\cos^{4t}\left(\frac{\pi k}{2N}\right)$ to make the integral of the whole expression easier to calculate. Secondly, we need to estimate the error of this integral approximation.

Notice that the e^{-2tx^2} is a good estimation of $\cos^{4t}(x)$

$$\begin{aligned}&e^{-2tx^2} - \cos^{4t}(x)\\ =&e^{-2tx^2} - e^{-2tx^2+O(tx^4)}\\ =&e^{-2tx^2}\left(1 - e^{O(tx^4)}\right)\\ \sim&\mathcal{O}\left(tx^4e^{-2tx^2}\right).\end{aligned} \tag{F3}$$

Substitute $\cos^{4t}\left(\frac{\pi k}{2N}\right)$ with $e^{-\frac{k^2\pi^2 t}{2N^2}}$ in Eq. (F15), we have

$$\begin{aligned}3\alpha^{\mathscr{L}}_{\{\gamma_i\gamma_j\},2t+1} &= -\frac{1}{N} + \frac{1}{N}\sum_{k=0}^{N-1}e^{-\frac{k^2\pi^2 t}{2N^2}}\left[\cos\left((i-j)\frac{k\pi}{N}\right) + \cos\left((i+j-1)\frac{k\pi}{N}\right)\right] + \mathcal{O}\left(e^{-\frac{\pi^2}{2}t}\right) &\text{(F4)}\\ &= -\frac{1}{N} + \frac{1}{N}\sum_{k=0}^{\infty}e^{-\frac{k^2\pi^2 t}{2N^2}}\left[\cos\left((i-j)\frac{k\pi}{N}\right) + \cos\left((i+j-1)\frac{k\pi}{N}\right)\right] + \mathcal{O}\left(e^{-\frac{\pi^2}{2}t}\right). &\text{(F5)}\end{aligned}$$

In the second line, we expand the summation to infinity, and it will not introduce much of errors because

$$\begin{aligned}\sum_{k=N}^{\infty} e^{-\frac{k^2\pi^2 t}{2N^2}} =& e^{-\frac{\pi^2}{2}t}\sum_{k=0}^{\infty} e^{-\frac{k^2\pi^2 t}{2N^2}}\\ \leq& e^{-\frac{\pi^2}{2}t}\sum_{k=0}^{\infty} e^{-\frac{k\pi^2 t}{2N^2}}\\ =& e^{-\frac{\pi^2}{2}t}\frac{e^{\frac{\pi^2 t}{2N^2}}}{e^{\frac{\pi^2 t}{2N^2}}-1}\\ =& \mathcal{O}\left(e^{-\frac{\pi^2}{2}t}\right)\end{aligned}$$

Lemma 6 did the second job, which turns the summation to the integral and evaluate the errors. Then, we could calculate the summation of series in Eq. (F5) via Lemma 6

$$3\alpha^{\mathscr{L}}_{\{\gamma_i\gamma_j\},2t+1} = \frac{1}{\sqrt{2\pi t}}(e^{-\frac{a^2}{2t}}+e^{-\frac{b^2}{2t}}) + \frac{2}{\sqrt{2\pi t}}(e^{-\frac{a^2+2N(N-a)}{2t}}+e^{-\frac{b^2+2N(N-b)}{2t}}) + \mathcal{O}\left(e^{-\frac{\pi^2}{2}t}\right), \tag{F6}$$

where a is defined as $|i-j|$ and b is defined as $i+j-1$. Here we absorb the error term given by Lemma 6 into the $\mathcal{O}\left(e^{-\frac{\pi^2}{2}t}\right)$ in Eq. (F5).

□

We can therefore conclude that the value of $\alpha^{\mathscr{L}}_{\{\gamma_i\gamma_j\},2t+1}$ will be on the order of $\frac{1}{\text{poly}(n)}$ if t is of the same order magnitude as a^2, $t=\Theta(a^2)$. Alternatively, if t is considered to be of lower order than a^2, as denoted by the little-o notation $t=o(a^2)$, then there exists an additional exponentially small term $e^{-\frac{a^2}{2t}}$ present in the expression for $\alpha^{\mathscr{L}}_{\{\gamma_i\gamma_j\},2t+1}$.

Lemma 5. *The expression of $\alpha^{\mathscr{L}}_{\{\gamma_i\gamma_j\},2t+1}$ could be simplified to the following form*

$$3\alpha^{\mathscr{L}}_{\{\gamma_i\gamma_j\},2t+1} = \frac{1}{N}+\frac{1}{N}\sum_k\left[\cos\left((i-j)\frac{k\pi}{N}\right)+\cos\left((i+j-1)\frac{k\pi}{N}\right)\right]\cos^{4t}\left(\frac{\pi k}{2N}\right). \tag{F7}$$

Proof. The lemma will be proved by directly calculation.

$$\begin{aligned}3\alpha^{\mathscr{L}}_{\{\gamma_i\gamma_j\},2t+1} =& \sum_\mu\left[\frac{1}{N}+\frac{2}{N}\sum_{k=1}^{N-1}\cos\left(\left(i-\frac{1}{2}\right)\frac{\pi k}{N}\right)\cos\left(\left(\mu-\frac{1}{2}\right)\frac{\pi k}{N}\right)\cos^{2t}\left(\frac{\pi k}{2N}\right)\right]\\ &\times\left[\frac{1}{N}+\frac{2}{N}\sum_{l=1}^{N-1}\cos\left(\left(j-\frac{1}{2}\right)\frac{\pi l}{N}\right)\cos\left(\left(\mu-\frac{1}{2}\right)\frac{\pi l}{N}\right)\cos^{2t}\left(\frac{\pi l}{2N}\right)\right]\\ =& 1/N+\frac{2}{N^2}\sum_k\left[\sum_\mu\cos\left(\left(\mu-\frac{1}{2}\right)\frac{\pi k}{N}\right)\right]\cos\left(\left(i-\frac{1}{2}\right)\frac{\pi k}{N}\right)\cos^{2t}\left(\frac{\pi k}{2N}\right) &\text{(F8)}\\ &+\frac{2}{N^2}\sum_l\left[\sum_\mu\cos\left(\left(\mu-\frac{1}{2}\right)\frac{\pi l}{N}\right)\right]\cos\left(\left(i-\frac{1}{2}\right)\frac{\pi l}{N}\right)\cos^{2t}\left(\frac{\pi l}{2N}\right) &\text{(F9)}\\ &+\frac{4}{N^2}\sum_{k,l=1}^{N-1}\sum_{\mu=1}^{N}\cos\left(\left(i-\frac{1}{2}\right)\frac{\pi k}{N}\right)\cos\left(\left(\mu-\frac{1}{2}\right)\frac{\pi k}{N}\right)\cos^{2t}\left(\frac{\pi k}{2N}\right)\\ &\times\cos\left(\left(j-\frac{1}{2}\right)\frac{\pi l}{N}\right)\cos\left(\left(\mu-\frac{1}{2}\right)\frac{\pi l}{N}\right)\cos^{2t}\left(\frac{\pi l}{2N}\right) &\text{(F10)}\end{aligned}$$

Notice that the summation of cosin function is zero

$$\begin{aligned}\sum_{\mu=1}^{N}\cos\left(\left(\mu-\frac{1}{2}\right)\frac{\pi k}{N}\right) &= -\frac{1}{2}\cos\left(\frac{1}{2}\pi(2k+1)\right)\csc\left(\frac{\pi k}{2N}\right)\\ &= \sin(k\pi)\csc\left(\frac{\pi k}{2N}\right)\\ &= 0.\end{aligned} \tag{F11}$$

Substitute this identity into Eq. (F10), we could eliminate the terms in line (F8) and (F9).

Also, notice that

$$\begin{aligned}&\sum_{\mu=1}^{N}\cos\left(\frac{\pi\left(\mu-\frac{1}{2}\right)i}{N}\right)\cos\left(\frac{\pi\left(\mu-\frac{1}{2}\right)j}{N}\right)\\ =&\frac{1}{2}\sum_{\mu=1}^{N}\cos\left(\frac{\pi\left(\mu-\frac{1}{2}\right)i}{N}-\frac{\pi\left(\mu-\frac{1}{2}\right)j}{N}\right)+\cos\left(\frac{\pi\left(\mu-\frac{1}{2}\right)i}{N}+\frac{\pi\left(\mu-\frac{1}{2}\right)j}{N}\right)\\ =&\frac{1}{2}\sum_{\mu=1}^{N}\cos\left(\frac{\pi(2\mu-1)(i-j)}{2N}\right)+\cos\left(\frac{\pi(2\mu-1)(i+j)}{2N}\right)\\ =&\frac{1}{4}\left(\sin(\pi(i+j))\csc\left(\frac{\pi(i+j)}{2N}\right)-\sin(\pi(j-i))\csc\left(\frac{\pi(i-j)}{2N}\right)\right).\end{aligned} \tag{F12}$$

This result gets value 0 when $\frac{\pi(i+j)}{2N}\neq a\pi$ or $\frac{\pi(i-j)}{2N}\neq b\pi$ for some integer a and b, because $\sin(\pi m)=0$. The term $\sin(\pi m)\csc\left(\frac{\pi m}{2N}\right)$ gets non-zero only when $\csc\left(\frac{\pi m}{2N}\right)$ gets infinity. Then, we could write down the conditions that i and j satisfy

$$\begin{cases} i+j=2aN \text{ or } |i-j|=2bN\\ a,b\in\mathbb{Z}\\ 1<i,j<N-1.\end{cases} \tag{F13}$$

The equation shows that the result is $j=k$. We can use L'Hôpital's rule to calculate the term

$$\lim_{x\to 0}\sin(\pi x)\csc\left(\frac{\pi x}{2N}\right)=2N \tag{F14}$$

when i and j satisfy the condition $i=j$. Plugin Eq. (F14) and Eq. (F12) into Eq. (F10), we have

$$\alpha^{\mathscr{L}}_{\{\gamma_i\gamma_j\},2t+1}=\frac{1}{N}+\frac{2}{N}\sum_{k}\cos\left(\left(i-\frac{1}{2}\right)\frac{\pi k}{N}\right)\cos\left(\left(j-\frac{1}{2}\right)\frac{\pi k}{N}\right)\cos^{4t}\left(\frac{\pi k}{2N}\right). \tag{F15}$$

Finally, we use trigonometric identities to expand this equation, thereby completing this proof

$$3\alpha^{\mathscr{L}}_{\{\gamma_i\gamma_j\},2t+1}=\frac{1}{N}+\frac{1}{N}\sum_{k}\left[\cos\left((i-j)\frac{k\pi}{N}\right)+\cos\left((i+j-1)\frac{k\pi}{N}\right)\right]\cos^{4t}\left(\frac{\pi k}{2N}\right). \tag{F16}$$

□

Lemma 6. *The result of summing the infinite series is*

$$\sum_{0}^{\infty}e^{-\frac{k^2\pi^2 t}{2N^2}}\cos\left(a\frac{\pi k}{N}\right)=\frac{N}{\sqrt{2\pi t}}e^{-\frac{a^2}{2t}}\left(1+2e^{-\frac{2N(N-a)}{t}}+\mathcal{O}(e^{-\frac{6N^2}{t}})\right)+\frac{1}{2} \tag{F17}$$

when $t<N^2$.

Proof. To aid analysis, we define a new function $f(k)$ that captures the pattern of each term, where $f(k)=e^{-\frac{1}{2}\beta^2k^2t}\cos(a\beta k)$ and $\beta:=\frac{\pi}{N}$. To determine the value of this infinite series, we invoke the Euler-Maclaurin formula. This formula relates the summation of a function to its integral representation, along with correction terms.

Specifically, the Euler-Maclaurin formula gives

$$\sum_{k=0}^{\infty} f(k) = \int_0^{\infty} f(x)dx + \frac{1}{2} + \int_0^{\infty} P_1(x)f'(x)\mathrm{d}x, \tag{F18}$$

where $P_1(x) = B_1(x - \lfloor x \rfloor)$, and B_1 is the first order Bernoulli polynomial

$$B_1 = x - \frac{1}{2}. \tag{F19}$$

By applying this formula, we can express the infinite series summation in terms of integrals, facilitating further analysis and solution of the problem.

Substitute the definition of B_1 into the Euler-Maclaurin expansion (F18), we have

$$\sum_{k=0}^{\infty} f(k) = \int_0^{\infty} f(x)\mathrm{d}x + \frac{1}{2} - \frac{1}{2}\int_0^{\infty} f'(x)\mathrm{d}x + \int_0^{\infty} (x - \lfloor x \rfloor)f'(x)\mathrm{d}x \tag{F20}$$

Integrating an serrate shape function can be relatively difficult. Therefore, we perform a Fourier transform on it,

$$x - \lfloor x \rfloor = \frac{1}{2} - \frac{1}{\pi}\sum_{k=1}^{\infty} \frac{1}{k}\sin(2\pi kx). \tag{F21}$$

changing the integral of the serrate shape function into an integral of trigonometric functions. This makes the calculation simpler.

By the definition of function f, the derivative of f could be calculated

$$f'(x) = -e^{-\frac{1}{2}tx^2\beta^2} tx\beta^2 \cos[ax\beta] - ae^{-\frac{1}{2}tx^2\beta^2}\beta \sin[ax\beta] \tag{F22}$$

$$= -tx\beta^2 f(x) - a\beta \tan(ax\beta)f(x). \tag{F23}$$

We utilize the symbolic computation platform Wolfram Mathematica to calculate the integral of $f(x)$

$$\int_0^{\infty} f(x)\mathrm{d}x = \frac{N}{\sqrt{2\pi t}} e^{-\frac{a^2}{2t}} \tag{F24}$$

and the integral of sin multiplied with $f'(x)$

$$\int_0^{\infty} \sin(2\pi kx)f'(x)\mathrm{d}x = -\frac{e^{-\frac{(2k\pi+a\beta)^2}{2t\beta^2}}\left(1 + e^{\frac{4ak\pi}{t\beta}}\right) k\pi^{\frac{3}{2}}}{\sqrt{2t\beta^2}}. \tag{F25}$$

Plugin Eq. (F23), Eq. (F25), and Eq. (F24) to Eq. (F20), we have

$$\sum_{0}^{\infty} f(n) = \int_0^{\infty} f(x)\mathrm{d}x + \frac{1}{2} + \sqrt{\frac{\pi}{2}}\sum_{k=1}^{\infty} \frac{e^{-\frac{(2k\pi+a\beta)^2}{2t\beta^2}}\left(1 + e^{\frac{4ak\pi}{t\beta}}\right)}{\sqrt{t\beta^2}} \tag{F26}$$

$$= \frac{N}{\sqrt{2\pi t}} e^{-\frac{a^2}{2t}} + \frac{1}{2} + N\sqrt{\frac{1}{2\pi t}}\left(\sum_{k=1}^{\infty} e^{-\frac{(2k\pi+a\beta)^2}{2t\beta^2}} + \sum_{k=1}^{\infty} e^{-\frac{(2k\pi-a\beta)^2}{2t\beta^2}}\right). \tag{F27}$$

Now, we want to estimate the order of the third term in Eq. (F27)

$$\sum_{k=1}^{\infty} e^{-\frac{(2k\pi+a\beta)^2}{2t\beta^2}} + \sum_{k=1}^{\infty} e^{-\frac{(2k\pi-a\beta)^2}{2t\beta^2}} \leq 2\sum_{k=1}^{\infty} e^{-\frac{(2k\pi-a\beta)^2}{2t\beta^2}} \tag{F28}$$

$$= 2e^{-\frac{a^2}{2t}} \sum_{k=1}^{\infty} e^{-\frac{2k^2N^2-2kaN}{t}} \tag{F29}$$

$$\leq 2e^{-\frac{a^2}{2t}+\frac{2aN}{t}} \sum_{k=1}^{\infty} e^{-\frac{2k^2N^2}{t}} \tag{F30}$$

$$= 2e^{-\frac{a^2}{2t}+\frac{2aN}{t}}\left(e^{-\frac{2N^2}{t}} + \mathcal{O}(e^{-\frac{6N^2}{t}})\right). \tag{F31}$$

If we consider t to be smaller in order than $\mathcal{O}(N^2)$, then we can view $e^{-\frac{6N^2}{t}}$ as a small number. Thus, the summation of $f(n)$ obtains the value

$$\sum_{0}^{\infty} f(n) = \frac{N}{\sqrt{2\pi t}} e^{-\frac{a^2}{2t}} \left(1 + 2e^{-\frac{2N(N-a)}{t}} + \mathcal{O}(e^{-\frac{6N^2}{t}})\right) + \frac{1}{2}. \tag{F32}$$

□

Appendix G: The relation between $\alpha^{\mathscr{L}}_{\{\gamma_i\gamma_j\},2t+1}$ and $\alpha^{\mathscr{R}}_{\{\gamma_i\gamma_j\},2t+1}$

Recall that we have divided the calculation of $\alpha_{\{\gamma_i\gamma_j\},2t+1}$ into two parts. One is the $\alpha^{\mathscr{L}}_{\{\gamma_i\gamma_j\},2t+1}$ and the other is $\alpha^{\mathscr{R}}_{\{\gamma_i\gamma_j\},2t+1}$. Theorem 1 gives the order of $\alpha^{\mathscr{L}}_{\{\gamma_i\gamma_j\},2t+1}$. In this section, we aim to bound the $\alpha^{\mathscr{R}}_{\{\gamma_i\gamma_j\},2t+1}$ by $\alpha^{\mathscr{L}}_{\{\gamma_i\gamma_j\},2t+1}$, so that the order of $\alpha_{\{\gamma_i\gamma_j\},2t+1}$ could be given by the $\alpha^{\mathscr{L}}_{\{\gamma_i\gamma_j\},2t+1}$.

We begin with the polynomial in Eq. (E24)

$$T^{(\text{whole})}_{\mathcal{P}_N}(t)(y_iy_j) = \sum_{\mu,\nu} \left(\mathscr{L}_{ij}(\mu,\nu,t)y_\mu y_\nu + \mathscr{R}_{ij}(\mu,\nu,t)y_\mu y_\nu\right). \tag{G1}$$

Then, we let the polynomial transform one time-interval step, and we get

$$\begin{aligned}
&T^{(\text{whole})}_{\mathcal{P}_N}(t+1)(y_iy_j) && \text{(G2)}\\
=&T^{(e)}_{\mathcal{P}_N} T^{(o)}_{\mathcal{P}_N}\left(T^{(\text{whole})}_{\mathcal{P}_N}(t)(y_iy_j)\right) && \text{(G3)}\\
=&\sum_{\mu,\nu} \left(\mathscr{L}_{ij}(\mu,\nu,t)(L(y_\mu)L(y_\nu) + R(y_\mu,y_\nu)) + \mathscr{R}_{ij}(\mu,\nu,t)(L(y_\mu)L(y_\nu) + R(y_\mu,y_\nu))\right) && \text{(G4)}\\
=&\sum_{\mu,\nu} \left(\mathscr{L}_{ij}(\mu,\nu,t)(L(y_\mu)L(y_\nu) + R(y_\mu,y_\nu)) + \mathscr{R}_{ij}(\mu,\nu,t)(L(y_\mu)L(y_\nu) + R(y_\mu,y_\nu))\right) && \text{(G5)}\\
=&\sum_{\mu,\nu} \mathscr{L}_{ij}(\mu,\nu,t+1)y_\mu y_\nu + \sum_{\mu,\nu} \mathscr{L}_{ij}(\mu,\nu,t)R(y_\mu,y_\nu)\\
&+ \sum_{\mu,\nu} \mathscr{R}_{ij}(\mu,\nu,t)(L(y_\mu)L(y_\nu) + R(y_\mu,y_\nu)). && \text{(G6)}
\end{aligned}$$

Deduce from Eq. (G1), we have

$$T^{(\text{whole})}_{\mathcal{P}_N}(t+1)(y_iy_j) = \sum_{\mu,\nu} \left(\mathscr{L}_{ij}(\mu,\nu,t+1)y_\mu y_\nu + \mathscr{R}_{ij}(\mu,\nu,t+1)y_\mu y_\nu\right). \tag{G7}$$

Compare Eq. (G6) and Eq. (G7), we have

$$\sum_{\mu,\nu} \mathscr{R}_{ij}(\mu,\nu,t+1)y_\mu y_\nu = \sum_{\mu,\nu} \mathscr{L}_{ij}(\mu,\nu,t)R(y_\mu,y_\nu) + \sum_{\mu,\nu} \mathscr{R}_{ij}(\mu,\nu,t)(L(y_\mu)L(y_\nu) + R(y_\mu,y_\nu)) \tag{G8}$$

$$\mathscr{R}_{ij}(l,k,t+1) = \sum_{\mu,\nu} \mathscr{R}_{ij}(\mu,\nu,t)\frac{\partial^2 L(y_\mu)L(y_\nu)}{\partial y_l \partial y_k} + \sum_{\mu,\nu} \left(\mathscr{L}_{ij}(\mu,\nu,t) + \mathscr{R}_{ij}(\mu,\nu,t)\right)\frac{\partial^2 R(y_\mu,y_\nu)}{\partial y_l \partial y_k}. \tag{G9}$$

Eq. (G9) describes the strict relationship between $\mathscr{R}_{ij}$ and $\mathscr{L}_{ij}$ in a recursive form, thereby giving the relationship between $\alpha^{\mathscr{L}}_{\{\gamma_i\gamma_j\},2t+1}$ and $\alpha^{\mathscr{R}}_{\{\gamma_i\gamma_j\},2t+1}$. However, deriving the general term formula from this recursive formula is difficult. Therefore, we hope to use some inequalities to simplify this recursive relationship and thus bound $\alpha^{\mathscr{R}}_{\{\gamma_i\gamma_j\},2t+1}$ by $\alpha^{\mathscr{L}}_{\{\gamma_i\gamma_j\},2t+1}$.

We will first define some auxiliary variables,

$$\alpha_k(t) := \frac{1}{2}\sum_{\mu=1}^{N-k}\left(\mathcal{L}_i(\mu,t)\mathcal{L}_j(\mu+k,t)+\mathcal{L}_i(\mu+k,t)\mathcal{L}_j(\mu,t)\right)$$
$$\beta_k(t) := \frac{1}{2}\sum_{\mu=1}^{N-k}\left(\mathscr{R}_{i,j}(\mu,\mu+k,t)+\mathscr{R}_{i,j}(\mu+k,\mu,t)\right)$$
$$a(t) := \begin{pmatrix}\alpha_0(t)\\ \alpha_1(t)\end{pmatrix}, \quad b(t) := \begin{pmatrix}\beta_0(t)\\ \beta_1(t)\end{pmatrix}.$$

Notice that $3\alpha^{\mathscr{L}}_{\{\gamma_i\gamma_j\},2t+1} = \alpha_0(t)$, $3\alpha^{\mathscr{R}}_{\{\gamma_i\gamma_j\},2t+1} = \beta_0(t)$. Because $\mathscr{L}_{i,j}(\mu,\nu,t)+\mathscr{R}_{i,j}(\mu,\nu,t)$ represents the probability of being in site y_iy_j during a random walk, it satisfies the property that the summation across all sites is 1. Meanwhile, the summation of all $\mathscr{L}_{i,j}(\mu,\nu,t)$ is 1. The two things deduce that

$$\sum_{\mu,\nu}\mathscr{R}_{i,j}(\mu,\nu,t) = 0. \tag{G10}$$

Especially, in numerical simulation, we observe that all $\mathscr{R}_{i,j}(\mu,\nu,t)$ are greater than 0 except for $\mu=\nu$. Under this assumption, we have the following theory:

Theorem 2 (same as Theorem **??**)**.** *Assume that* $\mathscr{R}_{i,j}(\mu,\mu,t) < 0$*, and* $\forall\mu\neq\nu$*,* $\mathscr{R}_{i,j}(\mu,\mu,t) > 0$*.* $-\beta_0(t) \le \frac{25}{72}\max_{k\ge0}\{\alpha_0(t-k)\}$.

Theorem 2 establishes the mathematical relationship between the two components $\alpha^{\mathscr{L}}_{\{\gamma_i\gamma_j\},2t+1}$ and $\alpha^{\mathscr{R}}_{\{\gamma_i\gamma_j\},2t+1}$. By combining this theoretical relationship with the equality described in Eq. (E30), we are able to deduce the order of magnitude of the $\alpha_{\{\gamma_i\gamma_j\},2t+1}$. Bringing these pieces together allows us to systematically determine the scale or size of $\alpha_{\{\gamma_i\gamma_j\},2t+1}$ based on the other defined quantities.

proof of theorem 2. From the recursive relationship in Eq. (G9) and Table **??**, we could write down the recursive relationship of β_k

$$\begin{aligned}\beta_0(t+1) \ge{}& \frac{6}{16}\beta_0(t)+\frac{8}{16}\beta_1(t)+\frac{2}{16}\beta_2(t)-\frac{14}{144}\left(\beta_0(t)+\alpha_0(t)\right)-\frac{1}{24}\left(\beta_1(t)+\alpha_1(t)\right)\\ &+\frac{4}{16}(\mathscr{R}_{ij}(0,0,t-1)+\mathscr{R}_{ij}(N,N,t-1))-\frac{1}{16}(\mathscr{R}_{ij}(0,1,t-1)+\mathscr{R}_{ij}(1,0,t-1))\\ &-\frac{1}{16}(\mathscr{R}_{ij}(N-1,N,t-1)+\mathscr{R}_{ij}(N,N-1,t-1))\\ \ge{}& \frac{5}{18}\beta_0(t)+\frac{11}{24}\beta_1(t)-\frac{7}{72}\alpha_0(t)-\frac{1}{12}\alpha_1(t) \qquad \text{(G11)}\\ \ge{}& \frac{5}{18}\beta_0(t)+\frac{5}{24}\beta_1(t)-\frac{7}{72}\alpha_0(t)-\frac{1}{12}\alpha_1(t) \qquad \text{(G12)}\end{aligned}$$

Here, we use the property that $\beta_0(t)+\alpha_0(t)$ is the summation of properties so that it is greater than 0 to inequality deflate the terms at the edges, like y_0y_0 or y_0y_1. Recall that we hold the assumption that $\mathscr{R}_{i,j}(\mu,\mu,t) < 0$, and $\forall\mu\neq\nu$, $\mathscr{R}_{i,j}(\mu,\mu,t) > 0$, so the edges terms of $\mathscr{R}_{ij}$ could be deflated out as well. Similarly, we have

$$\beta_1(t+1) \ge \frac{5}{9}\beta_0(t)+\frac{5}{12}\beta_1(t)+\frac{1}{18}\alpha_0(t)+\frac{1}{24}\alpha_1(t). \tag{G13}$$

Let β'_0 and β'_1 obtains the above recursive relation

$$\begin{cases}\beta'_0(t+1) = & \frac{5}{18}\beta_0(t)+\frac{5}{24}\beta_1(t)-\frac{7}{72}\alpha_0(t)-\frac{1}{12}\alpha_1(t)\\ \beta'_1(t+1) = & \frac{5}{9}\beta_0(t)+\frac{5}{12}\beta_1(t)+\frac{1}{18}\alpha_0(t)+\frac{1}{24}\alpha_1(t)\end{cases} \tag{G14}$$

with the same first term $\beta'_0(0)=\beta_0(0)$ and $\beta'_1(0)=\beta_1(0)$. The β and β' satisfy the relationship

$$\beta'_0(t) \ge \beta_0(t), \quad \beta'_1(t) \ge \beta_1(t). \tag{G15}$$

Similarly, we denote b' as $b'(t) := \binom{\beta'_0(t)}{\beta'_1(t)}$,

We rewrite the inequality groups (G14) to the matrix form

$$b'(t+1) = C_b b'(t) + C_a a(t), \quad \text{where} \tag{G16}$$

$$C_b = \begin{pmatrix} \frac{5}{18} & \frac{5}{24} \\ \frac{5}{9} & \frac{5}{12} \end{pmatrix}, \quad C_a = \begin{pmatrix} -\frac{7}{72} & -\frac{1}{12} \\ \frac{1}{18} & \frac{1}{24} \end{pmatrix}, \tag{G17}$$

and the matrices C_b and C_a govern these recursive dynamics. To solve this recursion explicitly, we diagonalize the C_b matrix. This allows us to express the recursion in closed form,

$$b'(t) = C_b^t b'(0) + \sum_{k=0}^{t-1} C_b^k C_a a(t-k-1). \tag{G18}$$

The term C_b^t could be calculated by eigenvalue decomposition $C_b = Q\Lambda Q^{-1}$, where $\Lambda = \text{diag}(\frac{25}{36}, 0)$. The eigenvector corresponding to $\frac{25}{36}$ is $(2, \frac{3}{2})^T$. This allows us to express C_b^k and $C_b^k C_a$ in terms of eigenvalues and eigenvectors

$$C_b^k = \left(\frac{5}{6}\right)^{2k} \begin{pmatrix} 2 & \frac{3}{2} \\ 0 & 0 \end{pmatrix} \tag{G19}$$

$$C_b^k C_a = \frac{1}{5}\left(\frac{5}{6}\right)^{2k} \begin{pmatrix} -\frac{1}{9} & -\frac{5}{48} \\ 0 & 0 \end{pmatrix} \tag{G20}$$

for any $k > 0$.

The variables we care about are α_0 and β_0 because they are directly related to the $\alpha^{\mathscr{L}}_{\{\gamma_i\gamma_j\},2t+1}$ and $\alpha^{\mathscr{R}}_{\{\gamma_i\gamma_j\},2t+1}$. Thus, we mainly consider the first item of $C_b^t b'(0)$ and $C_b^k C_a a(t-k-1)$, which could be expressed in the following form

$$C_b^k C_a a(t-k-1) = \lambda_k \alpha_0(t-k-1) + \eta_k \alpha_1(t-k-1). \tag{G21}$$

The λ_k and the η_k are coefficients

$$\begin{array}{ll} \lambda_k = -\frac{1}{45}\left(\frac{5}{6}\right)^{2k}, & \eta_k = -\frac{1}{48}\left(\frac{5}{6}\right)^{2k}, \quad \forall k > 0, \\ \lambda_0 = -\frac{7}{72}, & \eta_0 = -\frac{1}{12}. \end{array} \tag{G22}$$

Building on the previous relationships, we can now derive an explicit formula for $\beta_0'(t)$. From the expression for the first element of $C_b^k C_a a(t-k-1)$, we obtain

$$\beta_0'(t) = \sum_{k=0}^{t} \left(\lambda_k \alpha_0(t-k-1) + \eta_k \alpha_1(t-k-1)\right) \tag{G23}$$

We also know from the recursive relation of $\mathcal{L}_i$ that the state variables satisfy

$$\alpha_0(t+1) \geq \frac{3}{8}\alpha_0(t) + \frac{1}{2}\alpha_1(t). \tag{G24}$$

Leveraging this inequality into Eq. G23 allows us to place an upper bound on $\beta_0'(t)$

$$-\beta_0'(t) \leq -\sum_{k=1}^{t} \left(\lambda_k - \frac{3}{4}\eta_k + 2\eta_{k+1}\right) \alpha_0(t-k-1) + \frac{19}{72}\alpha_0(t) - \frac{1}{16}\alpha_0(t-1) \tag{G25}$$

$$\leq \sum_{k=1}^{t} \left(\frac{5}{6}\right)^{2k} \frac{307}{8640}\alpha_0(t-k-1) + \frac{19}{72}\alpha_0(t) - \frac{1}{16}\alpha_0(t-1) \tag{G26}$$

$$\leq \frac{25}{72} \max_{k\geq 0} \{\alpha_0(t-k)\} \tag{G27}$$

□

Appendix H: Efficiency when the distance of set is short

Proof. Let the initial tensor be P^S, and apply $T^{(\text{whole})}$ to the tensor P^S. Each $T^{(e)}T^{(o)}$ in $T^{(\text{whole})}$ will transform the P^S to the superposition of a series of Pauli tensors

$$T^{(e)}T^{(o)}P^S = \sum_{|S'|=|S|} \xi_{S'}|P^{S'}\rangle\rangle, \tag{H1}$$

where $\xi_{S'}$ are real coefficients that satisfy $\sum \xi_{S'} = 1$. Now, we only preserve the branches S' which has smaller distance $d(S') < d(S)$ unless $d(S) = 1$. The condition $d(S) = 1$ means that

$$P^S = \prod_{i\in\Lambda} Z_i \tag{H2}$$

via Jordan-Wigner transformation. Only the Pauli basis in the form of $\prod_{i\in\Lambda} Z_i$ have non-zero inner product with $|0,0\rangle\rangle$, which we explain it in Sec. E 2.

Table I tells us that summation of the coefficients of remained branches is greater than $\frac{1}{9^{|S|}}$. explain why is 1/9

We apply $T^{(e)}T^{(o)}$ $d(S)/2$-times, and in each step, only remain the branches with smaller cardinal numbers. Afterward, the summation of coefficients of remained branches is greater than $\frac{1}{9^{|S|d(S)/2}}$. Notice that $|S|$ is a constant number and $d(S) = \mathcal{O}(\log(n))$, the summation number is

$$\sum_{S''} \xi_{S''} \geq \frac{1}{9^{\mathcal{O}(\log(n))}} = \frac{1}{\mathcal{O}(\text{poly}(n))}, \tag{H3}$$

where S'' are the remained branches. □